



**Escola de Camins**  
Escola Tècnica Superior d'Enginyeria de Camins, Canals i Ports  
UPC BARCELONATECH

# Handling non-unique flows in macroscopic first-order intersection models by applying an equilibrium theory

Treball realitzat per:

**Pablo Sanz Tuñón**

Dirigit per:

**Chris Tampère, Raheleh Yahyamozdarani**

Màster en:

**Enginyeria de Camins, Canals i Ports**

Barcelona, 20/06/2021

Departament de Transport

**TREBALL FINAL DE MÀSTER**

## Table of content

1	Introduction.....	3
2	Problem statement .....	5
2.1	Building the feasible region.....	5
2.1.1	Non-negativity constraint.....	6
2.1.2	Demand constraint .....	6
2.1.3	Supply constraint .....	6
2.1.4	Priority ratio.....	7
2.2	Non-uniqueness root cause .....	8
2.2.1	Non-uniqueness example .....	8
2.2.2	Sufficient condition for non-uniqueness.....	9
3	A solution for non-unique transfer flows.....	11
3.1	Overview of the models .....	11
3.2	Equilibrium Theory in non-uniqueness problem .....	11
3.2.1	Equilibrium Theory mechanisms .....	11
3.2.2	Algorithm explanation .....	16
3.3	Solving remaining non-unique cases.....	20
3.3.1	Continuous-time Markov chain.....	20
3.3.2	Application in node model .....	21
3.3.3	Results from continuous-time Markov chain .....	24
4	Solution with proposed node model .....	27
5	Concluding remarks.....	31
6	Future work.....	32
7	Appendix .....	34
7.1	Appendix A .....	34
7.2	Appendix B .....	36
7.3	Appendix C .....	37
7.4	Appendix D .....	38
8	References.....	40

## 1 Introduction

Transport modeling is a broad field divided into static and dynamic traffic assignments. Dynamic Traffic Assignment (DTA) models are common traffic simulators that capture traffic dynamics such as time-varying flows or queuing processes. In DTA models, traffic is propagated by Dynamic Network Loading (DNL) models. Despite DNL models being widely implemented for various purposes, macroscopic DNL models that simulate the aggregate state of a network still present an issue of paramount importance that prevents a well-suited simulation in urban applications.

Macroscopic DNL models mainly consist of two components: link model and node model. A link model computes traffic flow dynamics through a certain distance (link) with homogenous characteristics. A node model connects links at intersections and respecting (1) the interactions among them and (2) other possible constraints imposed by the node itself (such as constraints coming from a traffic signal) estimate the number of vehicles that can pass through the intersection. Simple merge/diverge node models have already been a field of research (Daganzo, 1995; Jin and Zhang, 2003; Ni and Leonard, 2005; and Bar-Gera and Ahn, 2010), however, complex ones with multiple incoming and outgoing links are still under development (Lebacque, J., Khoshyaran, 2005; Gibb, 2011; Flötteröd and Rohde, 2011; Tampère et al., 2011; Corthout et al., 2012; Smits et al., 2015; and Jabari, 2016).

Corthout et al. (2012) discovered that under certain conditions (these conditions will be further discussed), different combinations of possible solutions might be observed in the real world, but current node models are not capable of considering this fact. The phenomenon of occurring different possible solutions is commonly denominated non-uniqueness. Neglecting multiple possible solutions can lead to unrealistic and misleading results and it is desirable to be included in the current node models, further discussed in more detail.

Non-uniqueness typically happens due to not complying with priority ratios *fully* or having one movement with different priority ratios in different conflict points at one intersection or both. For clarification, let's consider the unsignalized intersection shown in Figure 1. This intersection includes two incoming (or sending) links (links 1 and 2 of Figure 1) and four outgoing (or receiving) links (links 3,4,5 and 6 of Figure 1). Moreover, let's suppose that flows and road characteristics are fully symmetric to the vertical axis. A priori, if a node model computes these inputs under the assumption of fully complying with priority ratios, results obtained should also be symmetric. However, the situation can be more complicated in reality.

In the example of Figure 1, vehicles coming from incoming link 1 have priority over vehicles coming from incoming link 2. If vehicles originating from incoming link 1 do not fully comply with the priority ratios, they will block the other movement from incoming link 2, the inverse situation can be conceived too. In the real world, vehicles from the blocked direction will get aggressive and claim their priority so the other movement cannot do anything but yield. In total, over some time of observation both explained situations might happen regarding the level of congestion, politeness/aggressiveness of drivers, gap acceptance, etc. A desirable node model should be able to calculate the realistic combination of all the possible solutions over an arbitrary time rather than blindly combining them (in this example, resulting in a symmetric solution).

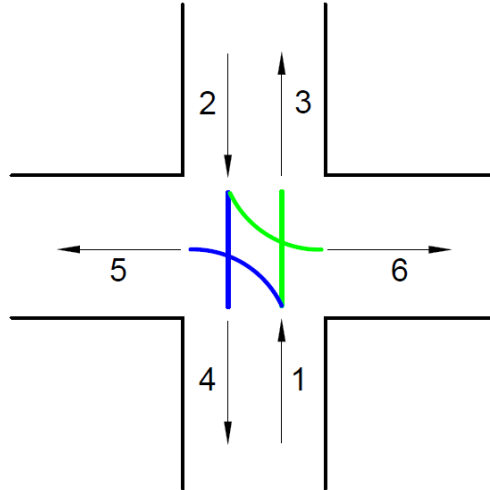


Figure 1. Intersection example

In front of this state-of-the-art problem in this master thesis, all the involved behavioral factors are assumed to be known<sup>1</sup> and goals are:

- Analyzing non-uniqueness root cause in detail and studying which traffic conditions are aiding it.
- Proposing and computing an Equilibrium Theory that eliminates unstable solutions from the feasible space.
- Proposing and computing a post-process model based on continuous-time Markov chain for combing the stable solutions found using the Equilibrium Theory.
- Providing several examples clarifying Equilibrium Theory's mechanism and efficiency.

The model presented in this study suits a case with a maximum of 2 incoming links and N outgoing links. Generalizing the model to higher dimensions (M-N dimensional) has been considered and it has been studied partially but not entirely in this research due to high complexity and lack of time. Nevertheless, some gained insights from Equilibrium Theory's generalization is provided in *Future work* section.

Finally, the short literature review provided should be justified. First of all, research on this topic is limited, and more importantly many of the existing ones are addressed by the Leuven mobility research center (L-Mob). Therefore, despite the short references section, it can be claimed that the state-of-the-art is known and related references have been included.

---

<sup>1</sup> Calibrating such a factor is possible through observations which is out of the scope of this research.

## 2 Problem statement

### 2.1 Building the feasible region

Before explaining the specific root cause producing non-uniqueness, it is first necessary to define the inputs, outputs, and mechanisms in a node model. A node could be defined as a connection between a set of incoming links and outgoing links. A node model distributes gaps among vehicles claiming it and eventually determines how many vehicles from which movement may occupy available gaps. The mechanism of this distribution process can be explained as an optimization problem from the user perspective, where flow is maximized respecting a set of constraints either coming from links (such as the limited amount of available gaps) or the node itself (such as the constraints imposed by a traffic signal).

To explain clearly which are constraints and how a node model works, the example of Figure 1 is considered. Turning the mentioned intersection into an optimization problem, we would obtain a 2D graph with axes  $q_1$  and  $q_2$  (see Figure 2). Space dimension depends on the number of movements that are connected to the node. If there are more than two incoming links, a plane with a higher dimension would be required. The number of outgoing links only determines the number of curves/lines constraining the solution space.

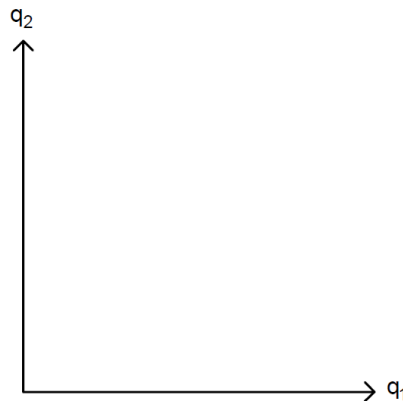


Figure 2.  $q_2 - q_1$  plane

During the next sections, the different types of constraints acting in this plane will be explained. The set of constraints will generate a feasible area or region, so the points located inside or at the edge of this area would be a feasible combination of flows.

Node model chooses a final solution regarding an objective function. This objective function is not unique in the literature, and different researches use different criteria such as Pareto optimal (Smits et al., 2015), flow maximizing (Jabari, 2016) or holding-free solution (Rohde, 2011; Tampère et al., 2011). In this thesis, the objective function chosen is the holding-free solution. The holding-free concept (or flow maximization from the user perspective) means that vehicles move as long as nothing stops them. In other words, for each combination of  $q_1$  and  $q_2$  only the solution lay on the boundaries of the feasible area can happen. This concept comes from the fact that road users try to optimize their own travel time selfishly so they seize any available opportunity in the outgoing link to pass through the intersection fast.

### 2.1.1 Non-negativity constraint

Flows can't be negative because they don't have a physical meaning. Thus, this constraint can be simply formulated as:

$$q_i \geq 0$$

For any incoming link  $i$ .

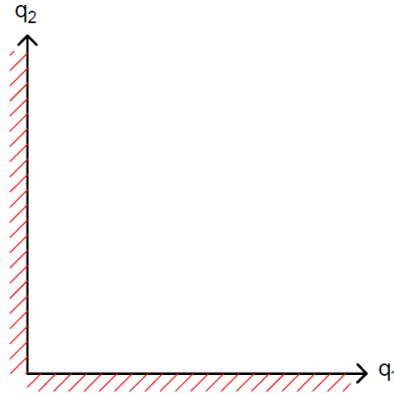


Figure 3.  $q_2 - q_1$  plane, adding non-negativity constraint

### 2.1.2 Demand constraint

Transfer flows can't be greater than the total flow available in the incoming link  $S_i$ . Then, each incoming link can transfer a certain maximum flow:

$$q_i \leq S_i$$

For any incoming link  $i$ .

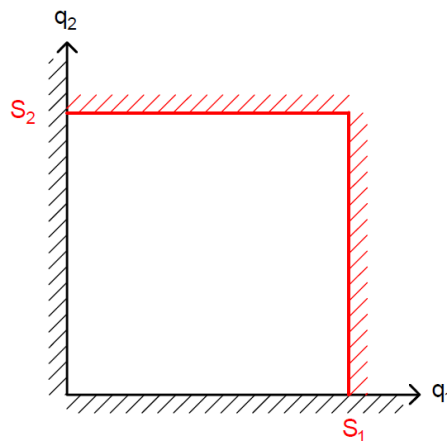


Figure 4.  $q_2 - q_1$  plane, adding demand constraints

### 2.1.3 Supply constraint

There are two types of supply constraints: internal and external. On the one hand, external supply constraints are limitations directly imposed by the outgoing links (i.e. the limited number of available gaps or the capacity of outgoing links). On the other

hand, internal supply constraints are produced by interactions between vehicles from different flows. For example, when two or more flows interact such that a few vehicles claim to occupy the same conflict point simultaneously but only one may.

Supply constraint can be expressed like the formula below, where  $F_{i,o}$  is a certain function representing the supply in a link or the potential capacity, depending if the supply is external or internal.

$$q_{i,o} \leq F_{i,o}$$

The non-uniqueness phenomenon can appear independently from which type of supply constraint is considered. Usually, in 2D intersections external supply constraints have a linear shape and internal supply constraints a convex shape. For generalization, in this document supply constraints will be represented as convex functions to represent that they can adopt any linear or convex shape (see Figure 5).

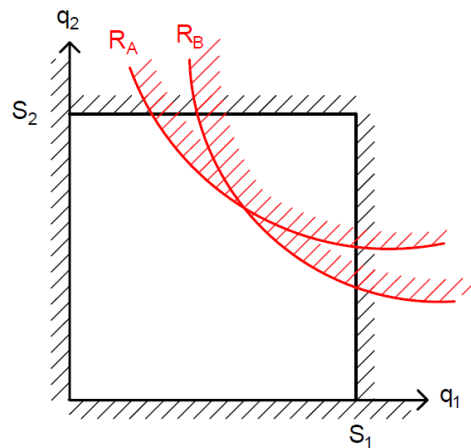


Figure 5.  $q_2 - q_1$  plane, adding supply constraints

#### 2.1.4 Priority ratio

Priority ratios application was an idea introduced by Daganzo (1995) to determine the proportion of scarce gaps occupied by different movements in congested cases. The simplest possible case is an intersection with two incoming links competing for transferring flow to a unique outgoing link (simple merge). If the sum of the available flow from both incoming links is greater than the capacity of the outgoing link, there are not enough inputs to decide how many vehicles should be transferred from each incoming link.

Daganzo (1995) proposed to give some weights (priority ratios) to the incoming links in order to decide which percentage of flow should be sent from each incoming link (or to decide what percentage of gaps can be occupied by which movement). In our 2D example, this concept is represented as a line departing from (0,0) with a certain slope ( $\frac{\alpha_2}{\alpha_1}$ ). The intersection of this priority ratio line (PRL) with the corresponding supply constraint (that supply constraint for which incoming links are competing) gives the result of the transfer flow. It is worth mentioning that in free-flow cases, the intersect of PRL and one of the  $S_1$  or  $S_2$  determines the solution.

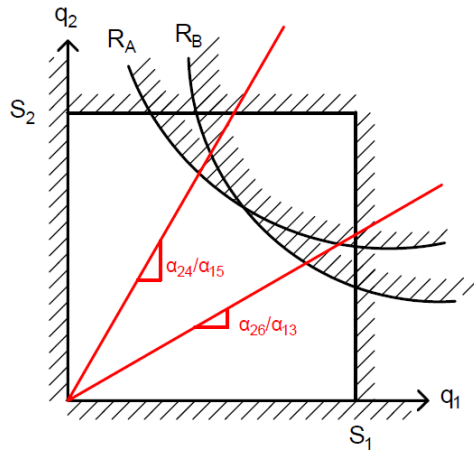


Figure 6.  $q_2 - q_1$  plane, adding PRLs

## 2.2 Non-uniqueness root cause

### 2.2.1 Non-uniqueness example

The priority ratio contribution from Daganzo (1995) determines the transfer flow proportion of each movement but it does not consider the fact that there can be more than one possible solution (non-uniqueness issue) because of not complying with the priority ratios in the real world. Corthout et al. (2012) discovered that in certain cases, non-uniqueness might appear even applying PRL: “When different priority ratios are used in a congested intersection in different conflict points for the same movement, uniqueness can’t be guaranteed. This non-uniqueness comes from two origins: turns yield to oncoming stream result in ambiguous priority and thus ambiguous order of solving procedure, or because the priority-on-the-right rule would cause difficulty in ranking priority”.

Let’s take an example to clarify why non-uniqueness can happen. Consider the intersection already showed in the first section of this document and represented again in Figure 7. On the one hand, incoming flow from link 1 has two possible options: going straight to link 3 or turning left to link 5. On the other hand, incoming flow from 2 has two available directions: keeping the direction and going through link 4 or turning left to link 6.

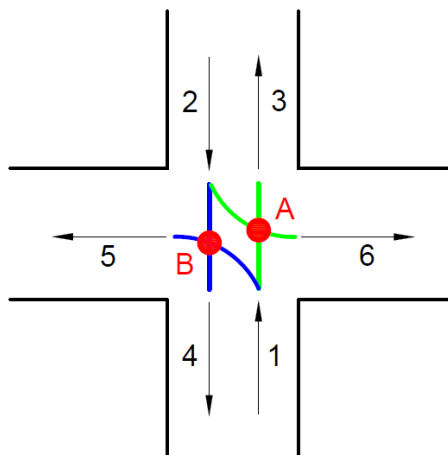


Figure 7. Intersection example

In this simple typical intersection, incoming link 1 has priority over incoming link 2 in conflict point A ( $P_{(1,3)} > P_{(2,6)}$ ) and has to yield in conflict point B ( $P_{(2,4)} > P_{(1,5)}$ ). If we start under the assumption that vehicles from incoming link 1 move blocking vehicles from incoming link 2, this means that the priority ratio at conflict B is not respected. After a while, blocked vehicles start to be impatient and claim their right of way at B. In this case, respecting the Conservation of Turning Fractions (CTF) principle<sup>1</sup> in addition to movement 1 → 5, movement 1 → 3 would also be blocked. In other words, the whole traffic flow from incoming link 1 would be blocked and the other flow can move. In both cases, priority ratios are partially respected, resulting in flipping from one situation to the other.

However, because of symmetry, the same reasoning could be applied for incoming link 2. In this case, all vehicles from link 2 would move initially, while vehicles from incoming link 1 would be blocked. Similar to the previous case after a while, the solution would swap to the other and so on. In conclusion, no matter we start with what assumption in this intersection two possible solutions could appear with the same initial boundary conditions<sup>2</sup> and there is not enough information to decide which one should be chosen. Notably, when supply is not scarce after a long enough time interval, all the vehicles would pass through the intersection and there is no complexity. All the complexity arise when there is not enough space for all the vehicles to pass and there will be a queue. Then, it matters to find a realistic combination of each possible solution to estimate a realistic queue length.

### 2.2.2 Sufficient condition for non-uniqueness

Regarding Corthout et al. (2012), a sufficient but not necessary condition for non-uniqueness is: “non-unique solutions for two flows  $q_i$  and  $q_{i'}$  are possible if the boundary conditions are such that a crossing or tangent point  $(\bar{q}_i, \bar{q}_{i'})$  exists between (at least) two (internal) supply constraints functions in which  $q_i$  and  $q_{i'}$  are mutually dependent and this point  $(\bar{q}_i, \bar{q}_{i'})$  lies within the feasible domain bounded by the demand constraints and the other supply constraints”. For an intersection point between an external supply in  $j$  and an internal supply in  $k$ , this condition can be expressed as:

$$\begin{aligned} \exists \bar{q}_i, \bar{q}_{i'}, j, k: \quad & \widehat{R}_j(\bar{q}_i, \bar{q}_{i'}) = \widehat{N}_k(\bar{q}_i, \bar{q}_{i'}) = 0 \\ & \text{with: } 0 < \bar{q}_i < S_i \\ & \quad \quad 0 < \bar{q}_{i'} < S_{i'} \\ & \widehat{R}_{j'}(\bar{q}_i, \bar{q}_{i'}) > 0 \quad \forall j' \neq j \\ & \widehat{N}_{k'}(\bar{q}_i, \bar{q}_{i'}) > 0 \quad \forall k' \neq k \end{aligned}$$

---

<sup>1</sup> CTF is equivalent with First-In-First-Out (FIFO) condition meaning vehicles that enter the link first should exit the link first. Now Based on CTF priciple if some vehicles wants to go towards one specific outgoing link bat had to stop, due to any constraint, other vehicles that do not want to go to the same outgoing link would also be blocked even if the other outgoing link includes free space. When movement 2 → 6 is stopped because movement 2 → 4 had to, respecting CTF principle; we write We express this idea as  $P_{(2,6)} \approx_{CTF} P_{(2,4)}$ .

<sup>2</sup> We did not mention what was the initial boundary conditions because they do not play a role in the reasoning.

The main idea behind this condition is that, if there is an intersection point between supply constraints in the feasible region, PRL can't decide a unique solution. Remember A and B points shown in Figure 7, they both decide for the solution if the curve of their constraint lies within the feasible region. If supply constraints do not intersect in the feasible region (see Figure 8), it means that one supply constraint is not active and therefore, it doesn't play any role in the flow transfer. For the example of Figure 7 this means, for instance, at every time instance more than one vehicle can be at A (or B) meaning that conflict point does not constrain the solution.

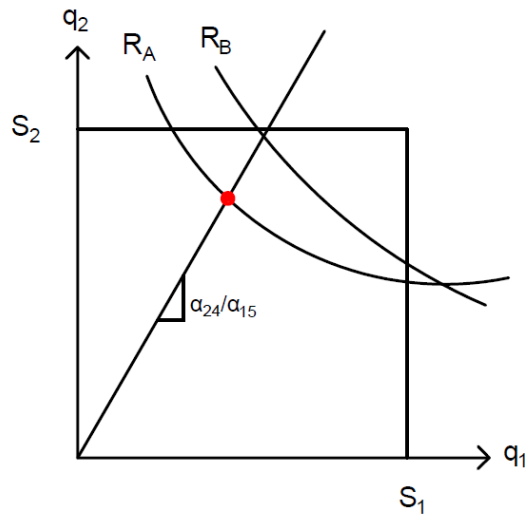


Figure 8. Intersection with a unique solution

However, when supply constraints intersect in the feasible region, both constraints are active and consequently two priority ratio lines can characterize the solution. In Figure 9, it can be observed how two PRLs can lead to a non-uniqueness case. If an intersection has at least two incoming links with a positive flow which are supply-constrained, bounded with one of the constraints associated with supply either being the available gaps in the outgoing link or a conflict point, non-uniqueness can occur.

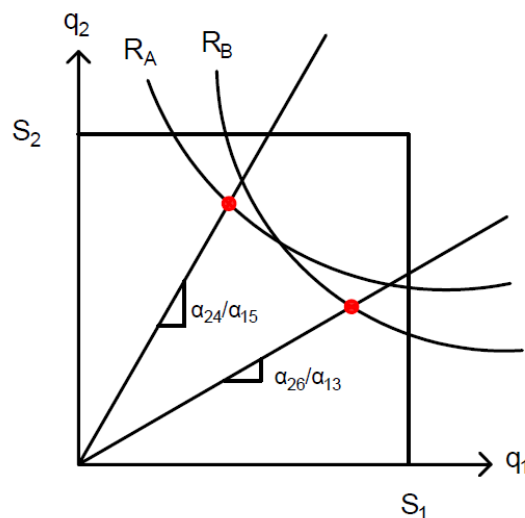


Figure 9. Intersection with non-unique solution

## 3 A solution for non-unique transfer flows

### 3.1 Overview of the models

This document presents two different methods to cope with non-unique solutions of a node model:

- Firstly, an Equilibrium Theory is proposed to distinguish between a case with different solutions and a case that *seemingly* has more than one solution. This is possible due to the behavior of drivers. For instance, when one movement is engaged in two conflict points and has the right-of-way in both, even if a few vehicles from the other movement(s) that should yield take the opportunity to enter the intersection, vehicles that have the right-of-way soon claim their right and the solution which allows the other movement(s) pass does not last (or is not stable). Non-stable solutions are not the interest and should be removed from the feasible solution's set. The equilibrium theory presented in *Equilibrium Theory* section filters solutions that are not stable. Then, if there is more than one stable solution, the following algorithm can be used to deal with non-uniqueness.
- Secondly, a new post-process approach is presented for coping with situations that have more than one stable solution. This approach combines in a realistic way the possibility of each solution happening such that one set of transfer flows can represent the state of a node. The combination procedure is based on the continuous Markov chains model and it is presented in *Solving remaining non-unique cases*.

To sum up, in cases where non-uniqueness is detected Equilibrium Theory will be applied. If after applying this theory non-uniqueness is solved, the final transferred flow is trivially obtained. Otherwise, the post-process approach will be applied to reach a unique solution.

### 3.2 Equilibrium Theory in non-uniqueness problem

#### 3.2.1 Equilibrium Theory mechanisms

Traditionally, the intersect point between PRLs and supply constraints has been considered a possible solution. As it has been already shown previously, when there are two active supply constraints PRLs can lead to having more than one possible solution (non-uniqueness). The Equilibrium Theory presented in this section faces the problem from another point of view: The intersect between a PRL and its corresponding supply constraint is not considered as a possible state, but as a potential one (called an attractor in the following).

Regarding the Equilibrium Theory presented here, a possible solution residing in the feasible region (the region constrained by demand and supply) may be an unstable one trying to reach stability or equilibrium by moving towards the attractor(s), *E* point in Figure 10. In fact, chevrons push any suboptimal solution to the optimal solution. Respecting the behavior of drivers, at least one constraint should bound the solution; otherwise, the solution suggests holding vehicles which is not realistic.

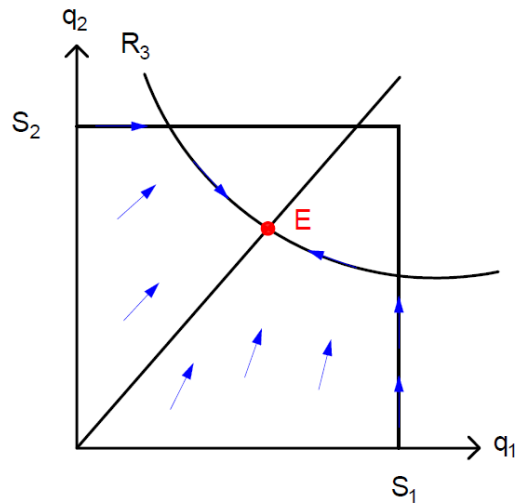


Figure 10. Equilibrium theory mechanism

Equilibrium Theory assumes that any point located in the envelope from the feasible region is a feasible potential flow (and not only the intersections between PRLs and supply constraints). However, these flows will be unstable except those attractors located on the boundary of the feasible area.

So far, we showed a line (PRL) in order to find attractors(s) but in reality, priority ratios  $\left(\frac{\alpha_i}{\alpha_{i'}}\right)$  are not constant over time and have a certain variability  $\frac{\alpha_i}{\alpha_{i'}} = f(t)$ . This variability comes from the fact that human behavior varies and some drivers may do not comply fully with the priority ratios. Considering PRL's variability allows solving cases that may truly have non-unique solutions.

All the points located in the boundary conditions cannot be a solution either. We clarify the point using an example: consider an intersection where two incoming links are competing for sending flow towards the same outgoing link. Flow  $q_2$  has priority over flow  $q_1$ , and the intersection between the PRL and the supply constraint ( $R_3$ ) gives an attractor  $E$  (see Figure 11).  $q_m$  and  $q_n$  are two flows located in the envelope of the feasible region (then, they are feasible flows) but they are not stable solutions and cannot be a member of the solution set. More specifically, if we start at  $q_m$ , regarding Equilibrium Theory we will not reside and we will be pushed to point  $E$  because  $q_m$  vehicles from  $q_2$  occupy a higher proportion of gaps than they may, respecting PRL. For a short while that may happen but soon there will be more aggressive drivers from  $q_1$  claiming their right or more polite drivers from  $q_2$  giving back the right to the other flow. In the end, the system resides where both flows can use their own right at  $E$ , maybe with a small variety over  $E$ , which is not the point of discussion now. This fact is taken into account introducing chevrons pointing to a stable solution. In the considered example of Figure 11 chevrons point at  $E$  from anywhere within the feasible area.

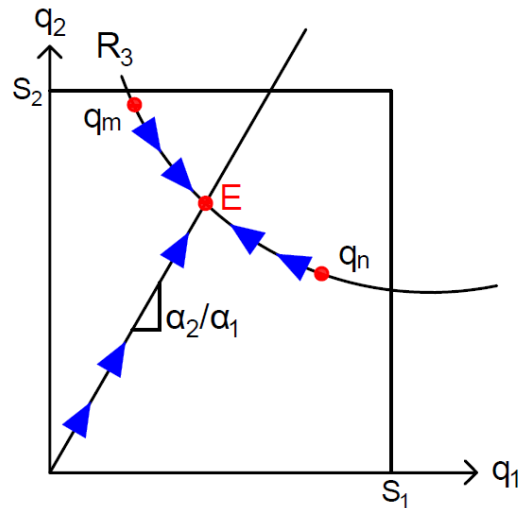


Figure 11. Driver behavior represented in the  $q_2 - q_1$  plane

When there is more than one supply constraint, PRL may intersect first with one and then with the other. In this case any PRL shows the priorities related to one of the constraints and more considerations are required respecting different types of intersection points that may occur:

- PRL first intersects with its corresponding supply constraint: the point is a stable point or an attractor.
- PRL first intersects with any other supply constraint: the point is not a stable point or an attractor because such a point does not have any behavioral definition.

Rather than an irrelevant supply constraint line PRL may intersect a demand line before a supply line too. For further clarification of this case, example of Figure 12 is considered which represents a simple merge intersection with two incoming links competing to send flow to the same outgoing link. As there is just one outgoing link, uniqueness is guaranteed (there is just one E point, and therefore all chevrons point to the same attractor). However, E point may or may not be the final solution:

- In Figure 12 (a), intersection between PRL and supply constraint generates the attractor  $E$  which is inside the feasible region. Flows along the envelope of the feasible region will try to reach equilibrium by moving towards  $E$  and, as there is not any other constraint preventing it, attractor  $E$  will be the final flow transferred  $q^*$ . In this case, congestion occurs because the supply constraint is active (bounds the solution).
- The situation presented in Figure 12 (b) is slightly different. In this case, the  $E$  point is located outside the feasible region and PRL first intersects with the demand line of  $q_1$  ( $S_1$ ). Again, since another constraint got active before the relevant supply constraint,  $E$  point cannot be a feasible attractor (or stable solution). Here chevrons starting from  $(S_1, 0)$  and  $(0, S_2)$  would push the solution from intersect point to another optimum point which is  $q^*$ . The intersect point is a suboptimal solution and does not satisfy the objective function. In this situation, incoming link 1 remains in free-flow regime because its demand is the active constraint and incoming link 2 would be congested because the supply bounds the flow from this link.

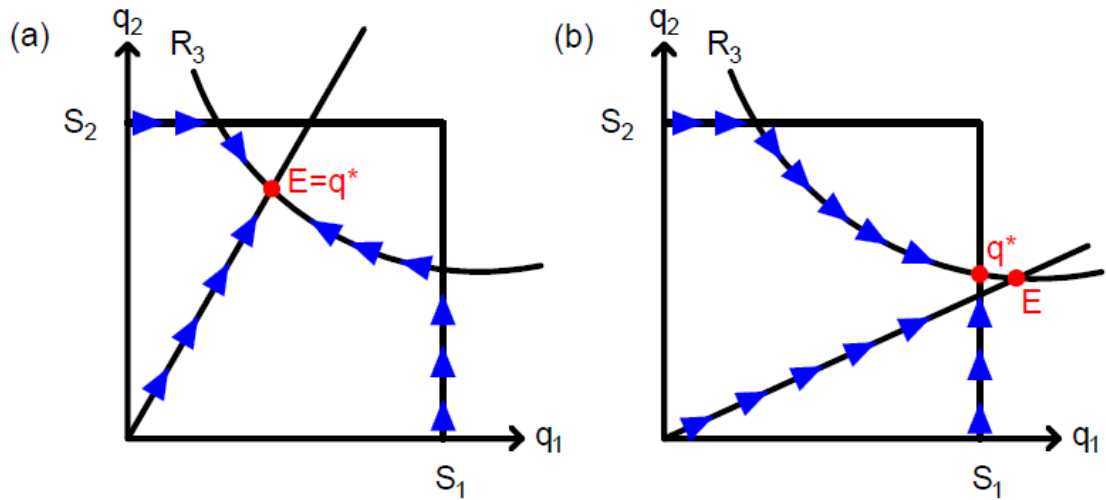


Figure 12. (a) PRL and supply constraint intersection occurs inside the feasible region; (b) PRL and supply constraint intersection occurs outside the feasible region

Now, let's observe how Equilibrium Theory is able to reach uniqueness in some non-unique situations for the traditional methods. Let's consider again the intersection from Figure 1. Equilibrium Theory states that attractors will be located in the intersection between PRL and its corresponding constraint, that is the intersection between  $\frac{\alpha_{24}}{\alpha_{15}}$  and  $R_3$  resulting the point  $E_3$ , and the intersection between  $\frac{\alpha_{26}}{\alpha_{13}}$  and  $R_4$  resulting the point  $E_4$  (see Figure 13 (b)). However, both are located beyond the feasible region. Then, the feasible solutions proposed by the traditional method are those intersections between the PRLs and the first supply constraint intersected, even if this supply constraint it's not its corresponding one. With these inputs, the traditional method would result in non-uniqueness with possible solutions being the red points shown in Figure 13 (a).

On the other hand, Equilibrium Theory mechanisms lead to uniqueness with the solution being  $q^*$ : chevrons pointing to  $E_3$  or  $E_4$  (depending on the supply constraint) converge in the intersection originated from both supply constraints.

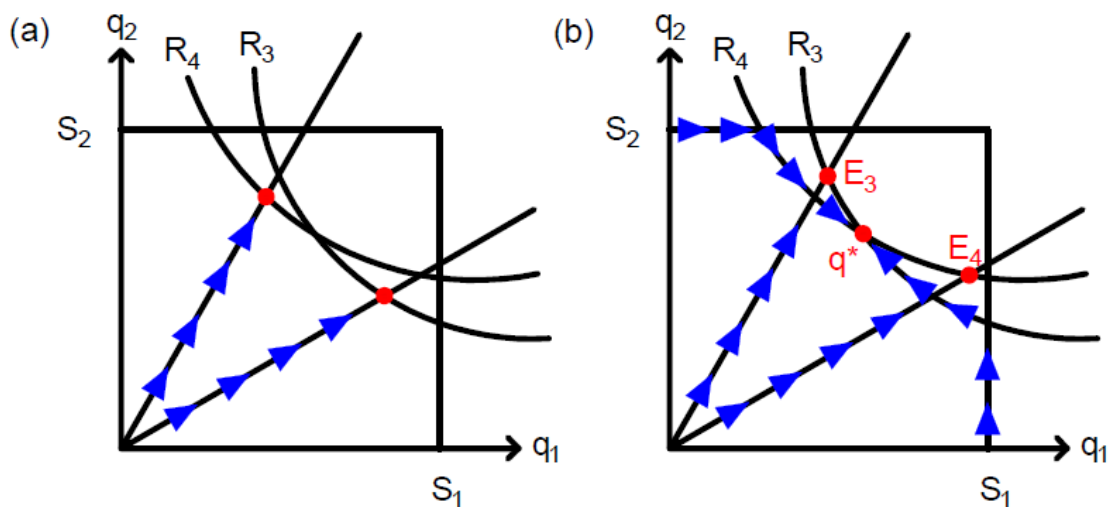


Figure 13. (a) Solution reach by traditional methods; (b) Solution reached by Equilibrium Theory

In Figure 14 (a) another situation is presented. The solution  $q^*$  from Equilibrium Theory corresponds to  $E_3$  attractor because: starting from point  $(S_1, 0)$ , chevrons move along the demand constraint until intersecting with  $R_3$  constraint. Then, chevrons point along the supply constraint to  $E_3$  and, as no constraint prevents them, they reach  $E_3$  point. Starting from point  $(0, S_2)$ , chevrons move along the demand constraint  $S_2$  until reaching  $R_4$ . Afterwards, chevrons along supply constraint  $R_4$  try to reach  $E_4$  attractor but this is not possible because  $R_3$  prevents it. Subsequently, chevrons continue along  $R_3$  constraint until reaching  $E_3$ .

Figure 14 (b) proposes an intersection with three outgoing links instead of two. Chevrons along  $R_4$  and  $R_5$  can't reach their E point because they are outside the feasible region. Nevertheless,  $E_3$  is located in the feasible envelope and then it becomes the solution  $q^*$ .

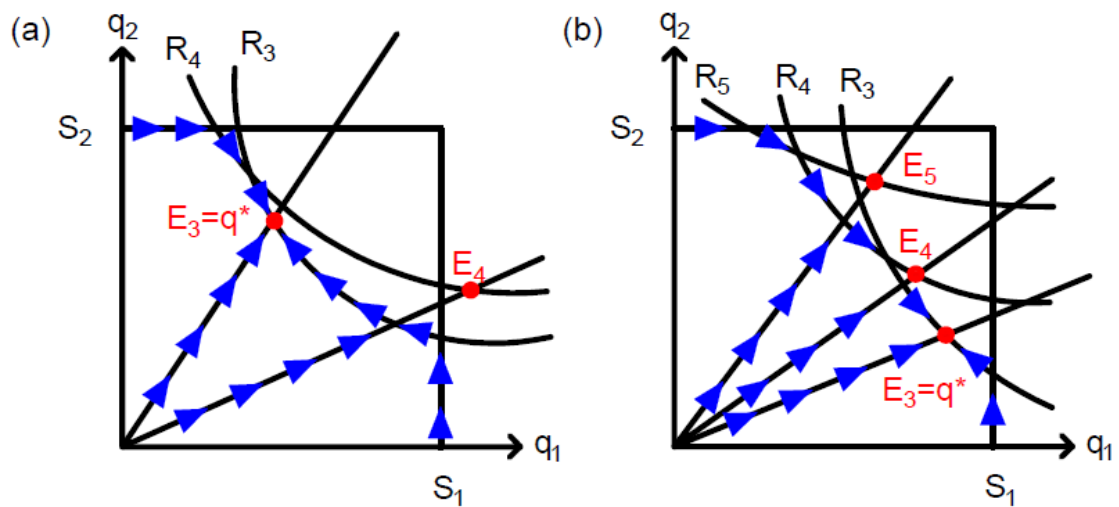


Figure 14. (a) Final flow transferred coincides with attractor  $E_3$ ; (b) Intersection with 3 outgoing links, final flow transferred coincides with attractor  $E_3$

As it was shown, many of the seemingly non-unique solutions of a node model can be avoided by implementing the proposed equilibrium theory. However, Equilibrium Theory does not always lead to uniqueness. Some non-unique cases can't be solved even applying these mechanisms. These situations occur when chevrons along the feasible region's envelope do not converge to the same solution and point to different E points. In other words, in these cases there exist more than one E attractor. In Figure 15 (a), an example of Equilibrium Theory resulting in non-uniqueness is shown. In this case, both attractors are located in the envelope of the feasible region, thus, chevrons point to two different E points both of which can be an attractor. Highlight that the intersection between supply constraints  $S$  is the point from the envelope which splits the orientation of chevrons: Those chevrons located in the left side of  $S$  point to  $E_3$  attractor, while those located to the right point to  $E_4$ .

Nevertheless, feasible solutions resulting from non-uniqueness do not always correspond with the E points. In some cases, non-uniqueness arises even when E points are outside the feasible region like in Figure 15 (b). In this case, chevrons can't reach E points because demand constraints  $S_1$  and  $S_2$  block them. Then, chevrons converge in  $q^*$  and  $q'$ , being these points the stable solutions proposed by the model.

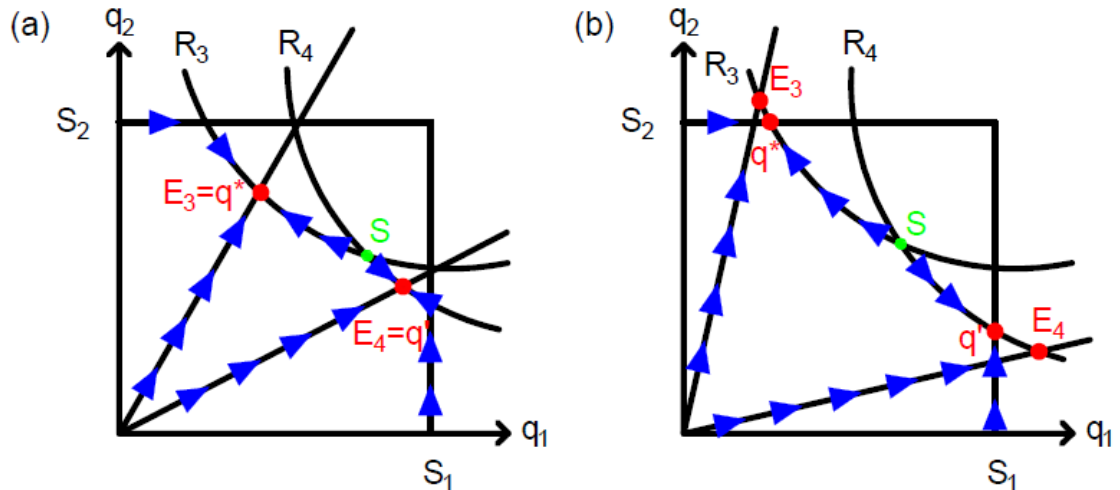


Figure 15. Examples of non-uniqueness once Equilibrium Theory has been performed. (a) Both attractors correspond with the feasible solutions; (b) One solution found do not correspond with an attractor

### 3.2.2 Algorithm explanation

Equilibrium Theory mechanisms have been conducted to solve any 2-N dimension problem (two incoming links, N outgoing links). This procedure could be split in 5 different parts:

1. Detect sufficient conditions for non-uniqueness
2. Compute intersections between constraints (demand and supply) and PRLs
3. Check feasibility of these intersections and create the feasible region
4. Define chevrons' direction and obtain stable solution(s)
5. Identify the set of stable solutions

The explanation of each part comes in the following with a graphical representation on the  $q_2 - q_1$  plane showing. For simplicity, we consider the intersection from Figure 1 in congested regime.

#### Detect sufficient conditions for non-uniqueness

Equilibrium Theory algorithm starts only when the sufficient conditions for having more than one possible solution are detected. As stated in *Sufficient condition for non-uniqueness* section, these conditions are:

- The intersection has two or more outgoing links (two or more supply resources that may bound the solution).
- At least, there are two active supply constraints. More specifically, feasible region is bounded by both supply constraints.

If these conditions are fulfilled, next steps of the algorithm will be computed. If not, uniqueness is guaranteed. In this example, the constraints' shapes are assumed as shown in Figure 16. As it fulfils non-uniqueness sufficient conditions (there are two outgoing links  $R_A, R_B$  and PRL intersects with the related supply constraint curve within the feasible area), Equilibrium Theory algorithm is computed.

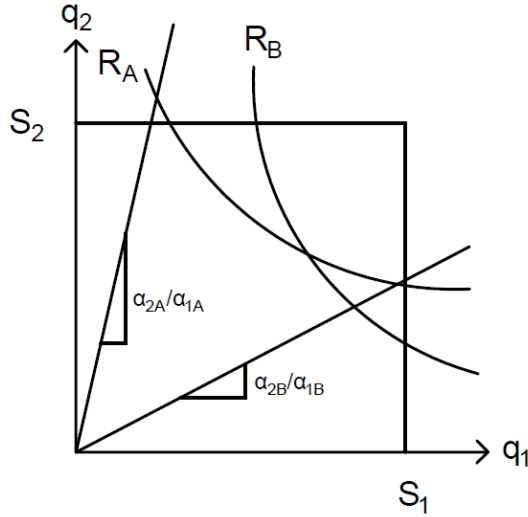


Figure 16. Intersection example with constraints and PRLs in the  $q_2 - q_1$  plane

### Compute intersections between constraints and PRLs

Intersections between constraints and intersections between PRLs and their corresponding supply constraints ( $E$  points) are the candidates for being stable solutions. In this way, a holding free solution is found.

By solving the system of equations representing constraints, the coordinates  $(q_1, q_2)$  of each intersection are obtained. The set of these intersections are those points with the potential of being a stable solution. Below, the solutions from the system of equations are showed and they are plotted in the  $q_2 - q_1$  plane in Figure 17.

Intersection between PRL  $\frac{\alpha_{2k}}{\alpha_{1k'}}$  and supply constraint  $R_j$ :

$$q_1 = \frac{R_j \alpha_{1k'}}{\alpha_{1k'} f_{1j} + \alpha_{2k} f_{2j}}$$

$$q_2 = \frac{q_1 \alpha_{2k}}{\alpha_{1k'}}$$

Intersection between PRL  $\frac{\alpha_{2k}}{\alpha_{1k'}}$  and demand constraint  $S_1$ :

$$q_1 = S_1$$

$$q_2 = \frac{S_1 \alpha_{2k}}{\alpha_{1k'}}$$

Intersection between PRL  $\frac{\alpha_{2k}}{\alpha_{1k'}}$  and demand constraint  $S_2$ :

$$q_1 = \frac{S_2 \alpha_{1k'}}{\alpha_{2k}}$$

$$q_2 = S_2$$

Intersection between supply constraints  $R_j$  and  $R_{j'}$ :

$$q_1 = \frac{R_j f_{2j'} - R_{j'} f_{2j}}{f_{1j} f_{2j'} - f_{1j'} f_{2j}}$$

$$q_2 = \frac{R_j - q_1 f_{1j}}{f_{2j}}$$

Intersection between supply constraint  $R_j$  and demand constraint  $S_1$ :

$$q_1 = S_1$$

$$q_2 = \frac{R_j - S_1 f_{1j}}{f_{2j}}$$

Intersection between supply constraint  $R_j$  and demand constraint  $S_2$ :

$$q_1 = \frac{R_j - S_2 f_{2j}}{f_{1j}}$$

$$q_2 = S_2$$

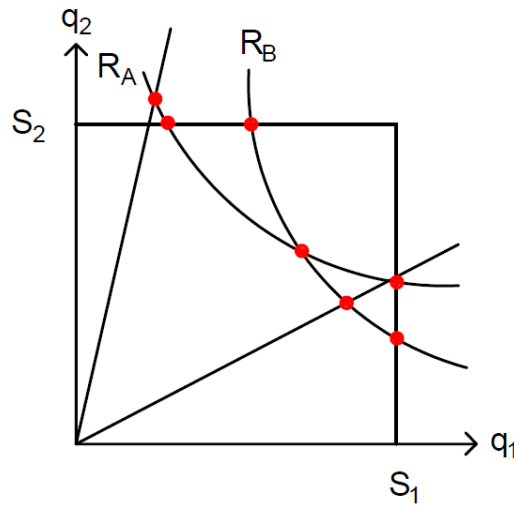


Figure 17. Candidates for being a stable solution

Check feasibility of these intersections and create the feasible region

Feasible points should respect all the constraints. For instance, the intersect point between  $R_A$  and the related PRL is not a possible solution since does not respect demand constraint line  $S_2$ . If a certain point fulfils all the existing constraints, then this point belongs to the feasible envelope. Considering the previous example, the points belonging to the feasible envelope are remarked in Figure 18.

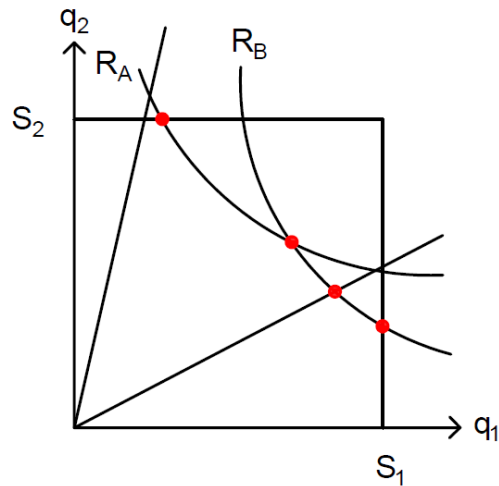


Figure 18. Intersection points belonging to the feasible region

Define chevrons' direction and obtain stable solution(s)

Next algorithm's step identifies chevrons' directions along the envelope of the feasible region. This process can be performed because firstly, we know which is the feasible envelope and secondly, we know where are the corners (members of the set that has been identified in the previous steps).

Stable solutions could be split in two categories bounded by either of demand or supply constraints. A demand constrained point follows the chevrons until it reaches a supply constraint (because of the holding-free assumption, the other direction will consume the part of gaps that could not be consumed by the demand constrained movement). Thus, a demand constrained point can only be stable if it intersects with a supply curve at the same point, otherwise, it is not stable.

To examine if a demand constrained point is a stable solution, the algorithm will check if the attractor is located inside or outside the feasible region:

- If attractor is located outside the feasible region: Chevrons will try to reach the attractor, but it won't be possible because demand constraint will block them. Thus, the intersection between the demand and the supply constraint will be a stable solution.
- If attractor is located inside the feasible region: Stable solution will be located along the supply constraint. Then, there is not any demand constrained stable solution.

Stable supply constrained solutions may exist when:

- A PRL intersects with its corresponding supply constraint inside the feasible region. This point is a stable solution.
- Two supply constraints intersect: As it has been demonstrated previously in Figure 14 (b), stable solutions can also be originated from the intersection of two supply constraints. Chevrons' direction will be obtained by observing their corresponding E points. If both chevrons converge to this intersection, this is a stable solution.

Applying these mechanisms in the previous example (Figure 18. Intersection points belonging to the feasible region Figure 18), we have one stable solution  $q^*$

bounded by demand constraint, and another  $q'$  which was the intersect point of  $R_B$  and the related PRL ( $\alpha_{2B}/\alpha_{1B}$ ).

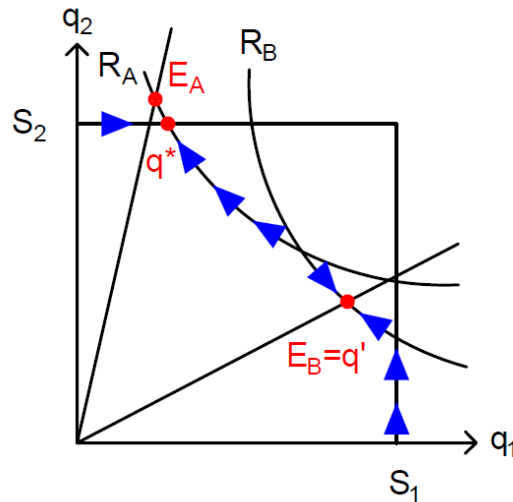


Figure 19. Application of chevrons along the envelope of the feasible region

### Identify the set of stable solutions

Once stable solution(s) are found using the concept of chevrons, either there is only one stable solution or more. The latter case, represents a situation in which non-uniqueness problem exists and the final solution of a node model shall be a realistic combination of all the stable solutions. In this study, a post-process model based on Markov change models is identified to find such a combination which is presented in the following.

## 3.3 Solving remaining non-unique cases

### 3.3.1 Continuous-time Markov chain

Traffic flow is a stochastic phenomenon and, subsequently, it can be described by a stochastic model. Markov chain is a stochastic model which describes a sequence of possible events in which the probability of each event depends only on the state of the previous event (the phenomenon is memoryless). It is possible to use a Markov model because in a road intersection, drivers' decisions are not affected by the past situations of the intersection; they will be only affected by the state of the road in the previous time step of study.

Moreover, it is important to highlight that the continuous-time Markov model is used and not the discrete Markov model. This is because in our case, the time spent in each state of the node is not constant. While in the discrete approach the transitions between events occur after a certain constant time  $\Delta t$ , continuous approach does not make this assumption and allows to calculate the time spent in each event.

More specifically, we define a continuous-time Markov chain as a random process  $\{X(t), t \in [0, \infty)\}$  in a countable state space  $S \subset \{0, 1, 2, \dots\}$ . If  $X(0) = i$ , then  $X(t)$  will stay in  $i$  for a random amount of time  $T_1$ , with  $T_1$  being a continuous random variable.

After this time  $T_1$ , the process will jump to a new state  $j$  during a random amount of time  $T_2$ . The probability of going from state  $i$  to state  $j$  is defined as  $p_{ij}$ . These times  $T_1, T_2 \dots$  are denominated holding times and follow an exponential distribution  $e^{-\lambda_i}$ . The memoryless behaviour of Markov chain can be expressed as:

$$P(X(t_{n+1}) = j \mid X(t_n) = i)$$

Proportions of time from being in each state given a certain time  $t$  are defined by the transition probability matrix  $P(t)$ . Thus, for an interconnected chain with dimension  $r$ , the transition probability matrix for any  $t \geq 0$  can be defined as:

$$P(t) = \begin{pmatrix} P_{11}(t) & \cdots & P_{1r}(t) \\ \vdots & \ddots & \vdots \\ P_{r1}(t) & \cdots & P_{rr}(t) \end{pmatrix}$$

In the continuous approach, the transition probability matrix must satisfy three different conditions:

- $P(0)$  is equal to the identity matrix.
- The sum of each row must be equal to 1.
- $P(s + t) = P(s)P(t) \quad \forall s, t \geq 0$ .

In practice, this transition matrix is usually obtained using the generator matrix  $G$ . Thus,  $P(t)$  is defined as:

$$P(t) = e^{tG}$$

Being  $G$  a matrix containing transition rates  $g_{ij}$  with value:

$$g_{ij} = \begin{cases} \lambda_i p_{ij} & \text{if } i \neq j \\ -\lambda_i & \text{if } i = j \end{cases}$$

And, the sum of each row from the generator matrix must be equal to 0.

### 3.3.2 Application in node model

Application of continuous-time Markov chain in node model can solve indetified non-unique situations. Each stable solution found by Equilibrium Theory will be a Markov state and holding times correspond with the time spent in each stable solution. The transition probability matrix  $P(t)$  define the proportion of time that traffic stays in each stable solution.

For the sake of simplicity, the following explanation focuses on the simplest case: the 2-2 dimensional case (2 incoming links and 2 outgoing links) with two stable solutions  $i$  and  $j$ . The transition probability matrix is defined as:

$$P(t) = \begin{pmatrix} P_{ii}(t) & P_{ij}(t) \\ P_{ji}(t) & P_{jj}(t) \end{pmatrix}$$

Then, the generator matrix  $G$  is a 2x2 matrix. Assuming two positive variables  $\alpha, \beta > 0$ :

$$G = \begin{pmatrix} -\alpha & \alpha \\ \beta & -\beta \end{pmatrix}$$

Knowing that  $P(t) = e^{tG}$ , transition probability matrix can be defined in function of  $\alpha$  and  $\beta$  variables:

$$P(t) = \begin{pmatrix} \frac{\beta}{\alpha + \beta} + \frac{\alpha}{\alpha + \beta} e^{-(\alpha + \beta)t} & \frac{\alpha}{\alpha + \beta} - \frac{\alpha}{\alpha + \beta} e^{-(\alpha + \beta)t} \\ \frac{\beta}{\alpha + \beta} - \frac{\beta}{\alpha + \beta} e^{-(\alpha + \beta)t} & \frac{\alpha}{\alpha + \beta} + \frac{\beta}{\alpha + \beta} e^{-(\alpha + \beta)t} \end{pmatrix}$$

$\alpha$  and  $\beta$  are variables which define the willingness of making a transition from one state to another. For the node model application,  $\alpha$  and  $\beta$  include information about the drivers' characteristics (because drivers can make a transition from one state to the other) and also factors such as arrival pattern, aggressiveness and politeness behaviors from drivers, collisions or other unexpected phenomena, randomness, etc. In general, any factor that can have an impact on making a transition or not is included in  $\alpha$  and  $\beta$  which can be calibrated by observations, but this is not the scope of this study.

Let us consider the unsolved non-uniqueness case from *Equilibrium Theory*. After applying the Equilibrium Theory algorithm, two stable solutions  $q^*$  and  $q'$  remained. In reality, traffic flow is not a deterministic phenomenon but a stochastic one in which distributions characterizing different phenomena may also vary over time. Therefore, the solution of a node model is not deterministic either and has a variation from the expected value (the solution that has been found so far). It can also be said that, the slope of each PRL ( $\frac{\alpha_2}{\alpha_1 q^*}$  or  $\frac{\alpha_2}{\alpha_1 q'}$  for each case) has a distribution around the expected values shown in Figure 20.

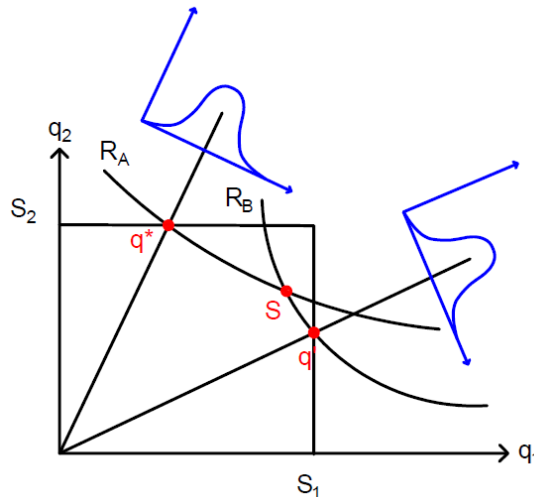


Figure 20. Traffic flow distribution for each stable solution

In addition, as it was previously mentioned, all the chevrons located to the left side of  $S$  point to the  $q^*$  solution while, the chevrons located to the right side of  $S$  point to  $q'$  solution (see Figure 21). Thus,  $S$  point becomes the frontier between both stable

solutions. As a result, it can be said that if traffic conditions moves the solution from one of the stable solutions to the  $S$  point, the transition to the other solution would be possible.

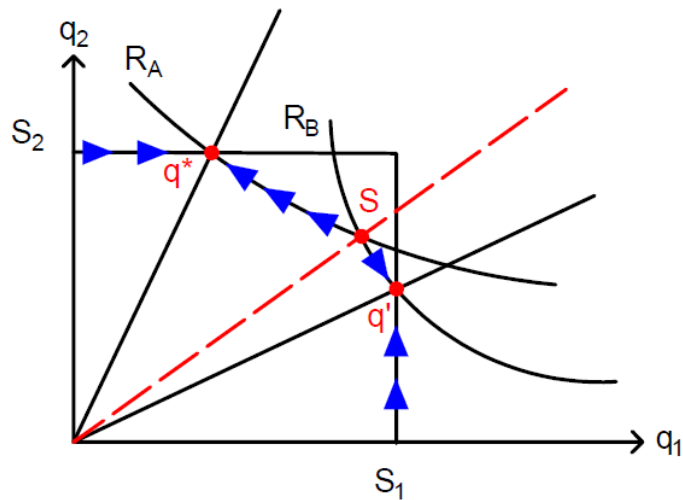


Figure 21. Chevrons direction depends from flow distribution

Then, the distance between a stable solution and the intersection between supply constraints becomes relevant because it will determine the easiness of making a transition. The closer the stable solution is to  $S$ , the greater the chances of making a transition.

Willingness of performing a transition is determined by introducing the slope of  $S$  point in the distribution functions from Figure 20. The outer area from the functions will represent  $\alpha$  and  $\beta$  variables (see shaded areas in Figure 22). Notice that if  $S$  slope move away from stable solution's slope  $\alpha$  and  $\beta$  decrease. On the contrary, if it moves closer willingness of making a transition increases.

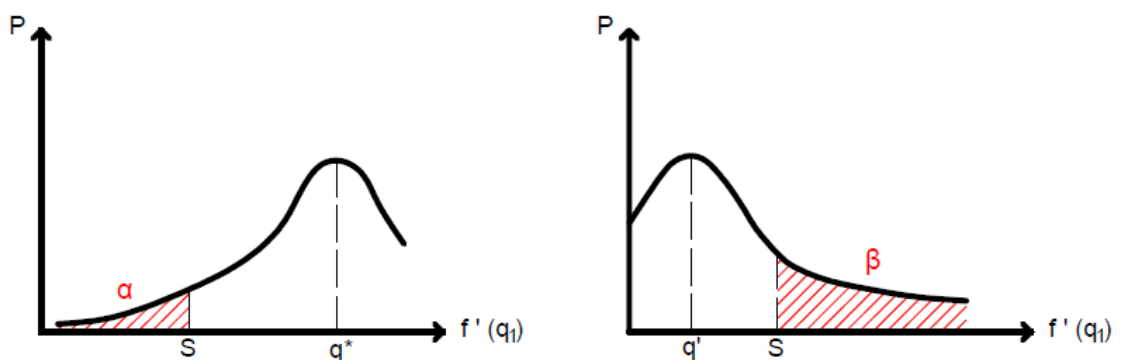


Figure 22. Normal distribution functions of stable solutions' slope

Once  $\alpha$  and  $\beta$  variables are determined, the probability matrix  $P(t)$  can be computed. For a given time  $t$ , remember that  $P(t)$  components are considered as the proportion of time that traffic stays in each stable solution. Thus, if for example the current state is  $i$ , the probable residual time at  $i$  during the next period of time  $t$  is  $tP_{ii}$  and the probable residual time at  $j$  state is  $tP_{ij}$ . Following the same reasoning, if the

starting state is  $j$ , during the next period of time  $t$  the probable residual time at  $i$  and  $j$  respectively are  $tP_{ji}$  and  $tP_{jj}$ .

Uniqueness will be reached by applying a weighted average between both stable solutions, with weights being the components of  $P(t)$  matrix. The result from the average expected flow is denominated  $K(K_1, K_2)$  as shown in Figure 23. Note that  $K$  is closer to  $q^*$  than to  $q'$  because making a transition from  $q^*$  to  $q'$  is considerably less probable than backwards.

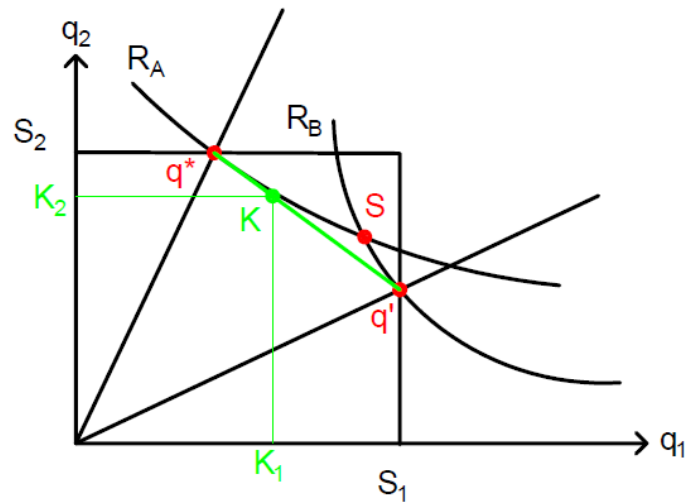


Figure 23. Weighted average performed from both stable solutions

### 3.3.3 Results from continuous-time Markov chain

Some results are shown after applying the proposed continuous-time Markov chain on an example with two stable solutions. These outputs allow observing how the model reacts to constraints modifications and traffic priority changes. Suppose that after implementing the Equilibrium Theory algorithm, an intersection gives the following  $q_2 - q_1$  plane resulting in non-uniqueness with  $q^* (2,8)$ ,  $q' (8,5)$  and  $S (6,6)$  points shown in Figure 24.

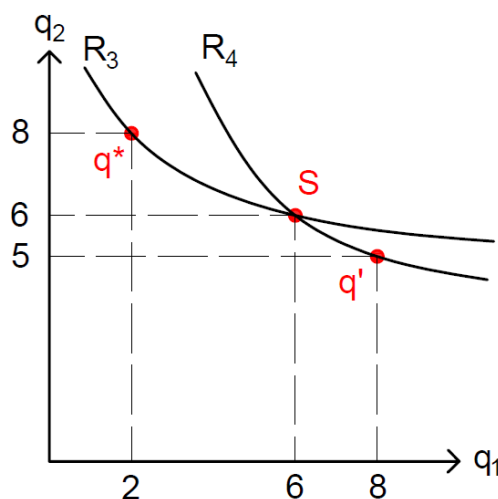


Figure 24. Non-uniqueness example 1

It can be seen that  $q'$  is closer to  $S$  than  $q^*$ . Thus, over a certain time,  $q^*$  should be more frequent than  $q'$  due to the more difficulties for making a transition from  $q^*$  to the other.

Let us analyse the results obtained from applying continuous-time Markov chain, assuming that there is a normal distribution function over the stable solutions with mean equal to the stable solution and standard deviation equal to 3. Plotting the components of the transition probability matrix  $P(t)$  for different time periods, these are the values obtained:

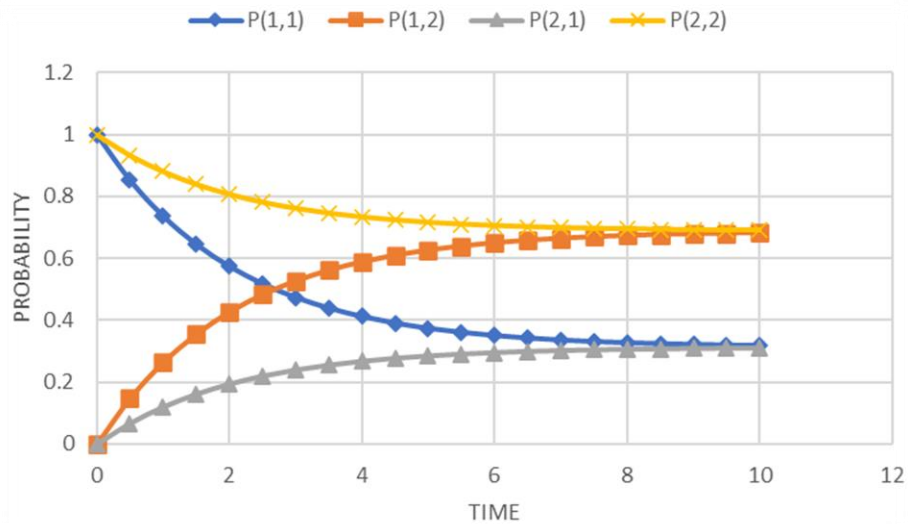


Figure 25. Transition probability matrix results from example 1

To be able to analyse correctly Figure 25, the meaning of each component from the transition probability matrix should be clear. This meaning can be summed up as:

- $P_{11}$ : staying in stable solution  $q'$
- $P_{12}$ : making a transition from  $q'$  to  $q^*$
- $P_{21}$ : making a transition from  $q^*$  to  $q'$
- $P_{22}$ : staying in stable solution  $q^*$

Let's focus on time  $t = 0$  in Figure 25. If there is no passing of time, the probability of staying in the starting state is 100% while probability of making a transition is 0%. However, if  $t = \infty$  components from the matrix converge to certain values, which means that for longer time periods the impact of the starting state is negligible. In this example 1,  $P_{12}$  and  $P_{22}$  converge to 0.68 while  $P_{11}$  and  $P_{21}$  converge to 0.32. Then, it can be concluded that for longer periods of time, traffic flows with amounts representing  $q^*$  68% of the time and with amounts representing  $q'$  for the remaining 32% of the time.

Now, let's consider another 2-2 dimension intersection with different constraints and flow inputs. The traffic scenario observed can be translated in the  $q_2 - q_1$  plane like the one presented in Figure 26.

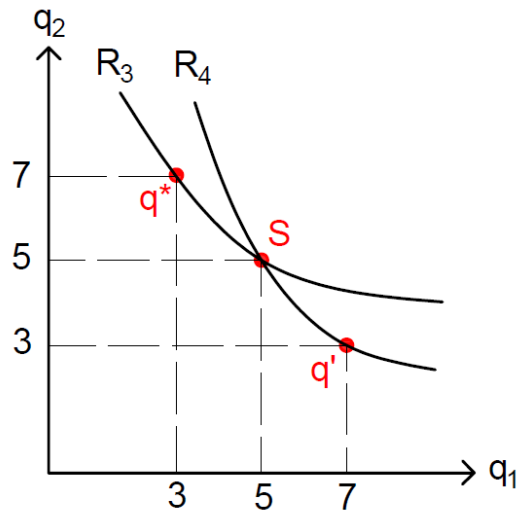


Figure 26. Non-uniqueness example 2

The main difference from this example compared with the previous one is that in this case, the distance between each stable solution and the intersection  $S$  is equal (notice about  $q^*$  and  $q'$  coordinates respect to the  $S$  point). Then, the probability of making a transition should be the same for both solutions. Plotting the results from the transition probability matrix assuming the same distribution function as the previous example, the values obtained are represented below:

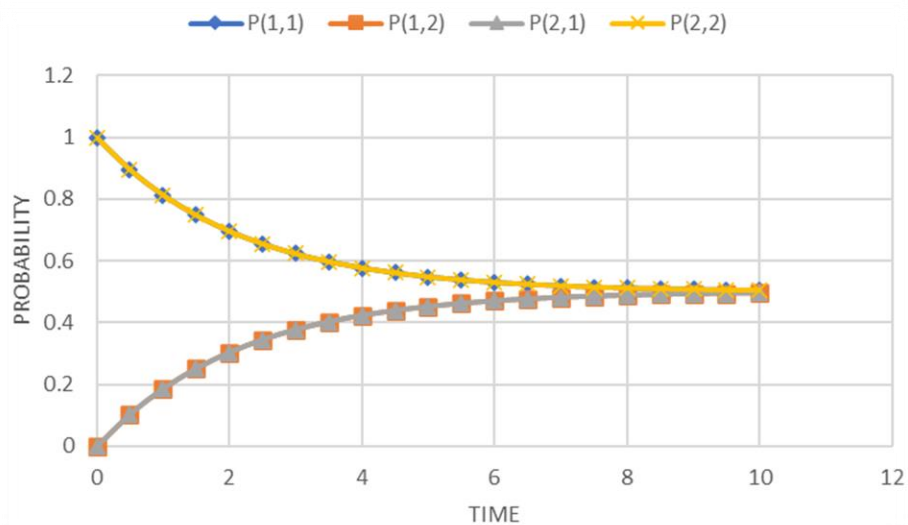


Figure 27. Transition probability matrix results from example 2

As expected, in this second example all components from the matrix  $P(t)$  converge to the same value, specifically to 0.5. These results confirm the first assumption: for equidistant states considering  $t = \infty$ , there is 50% chance of being in each state independently from the starting state.

## 4 Solution with proposed node model

The key contribution from this model is the ability to observe the complete set of feasible solutions, and then to select an appropriate weighted average according Markov chain. Considering all the possible solutions gives a more realistic approximation. However, traditional node model just chooses one solution from all the feasible ones.

This difference will be demonstrated comparing the traditional and the proposed node model in a real scenario. For it, the intersection represented in Figure 28. Intersection proposed for the models comparison will be modelled. This sketch has two corridors 1 and 2 adding flow to the intersection from the south and north side respectively, and two other corridors 3 and 4 pointing outwards the intersection to the west and east. Each corridor is 10km long and it has been decomposed by links with 0.5km distance. Therefore, the model is made up by 40 links, 10 in each corridor.

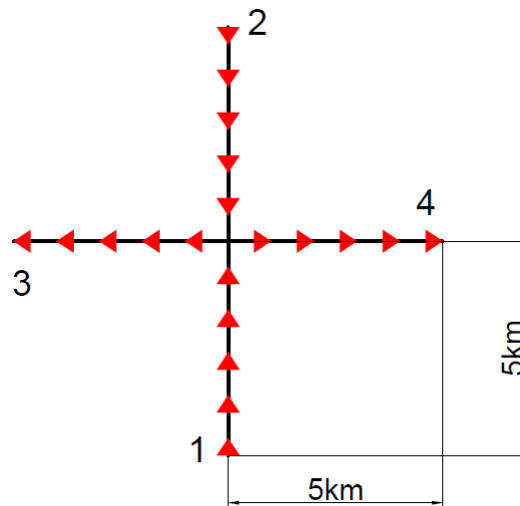


Figure 28. Intersection proposed for the models comparison

Both incoming flows 1 and 2 can turn either left or right. In congestion regime, this intersection sketch could induce to cyclic priority:  $P_{(1,4)} > P_{(2,4)}$  because priority-to-the-right rule,  $P_{(2,4)}$  blocks  $P_{(2,3)}$  because FIFO rule,  $P_{(2,3)} > P_{(1,3)}$  and  $P_{(1,3)}$  blocks  $P_{(1,4)}$ . Incoming flow and link characteristics like capacity of the road, maximum free speed or maximum density (see Table 1) are set in a way that congestion regime is guaranteed during almost all the simulation time. Thus, incoming links 1 and 2 compete for sending flow to 3 and 4. This competition is also determined by the priorities and turning fractions parameters, which are showed in Table 2.

Table 1. Road characteristing from the model

Corridor	Road capacity (veh/h)	Free speed (km/h)	Jam density (veh/km)
1	3000	120	200
2	3000	120	200
3	2000	80	150
4	2000	80	150

Table 2. Priority ratios and turning fractions imposed in the intersection

Origin-destination	Priority ratios	Turning fractions
1 → 3	0.2	0.4
1 → 4	0.8	0.6
2 → 3	0.8	0.65
2 → 4	0.2	0.35

Assuming these inputs, incoming links will be most of the time saturated and therefore, the available sending flow will be equal to the capacity of these incoming links. Figure 29. Demand and supply constraints represented in  $q_2-q_1$  plane in congestion regime plots the traffic scenario in congested regime in the  $q_2 - q_1$  plane.

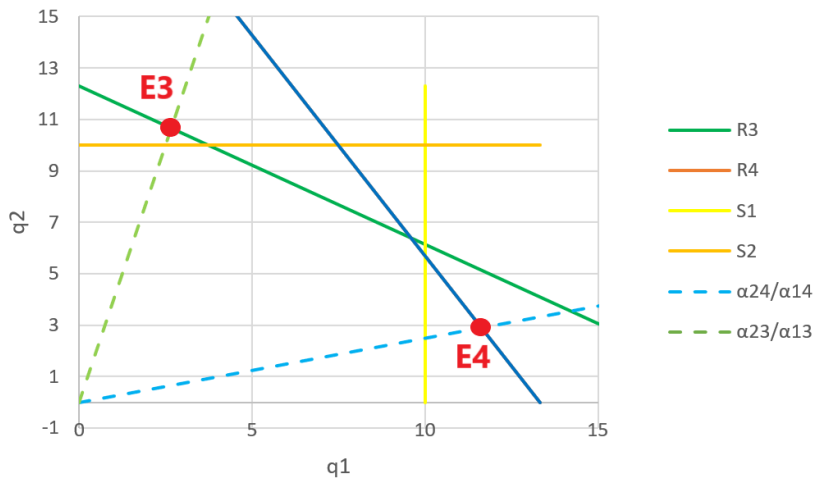


Figure 29. Demand and supply constraints represented in  $q_2 - q_1$  plane in congestion regime

Traditional node model and proposed node model with Equilibrium Theory give different solutions. On the one hand, traditional model suggests the  $S$  intersection between supply constraints as the final solution because of the holding-free criteria. On the other hand, equilibrium theory mechanisms detects two stable solutions  $A$  and  $B$  and performs a weighed average between both points according to the transition probability matrix from Markov. As observed in Figure 30 and Figure 31, traditional node model is blind with the real situation:  $q_2 - q_1$  plane presents three possible solutions  $A$ ,  $B$  and  $S$  and just one is considered.

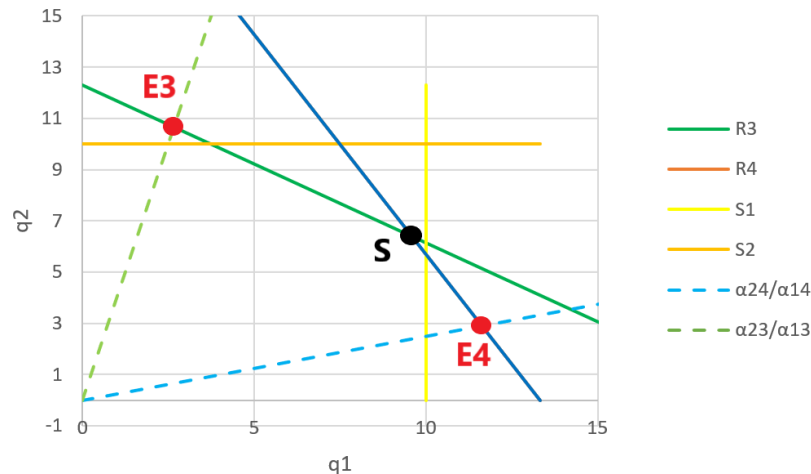


Figure 30. Solution proposed by traditional node model

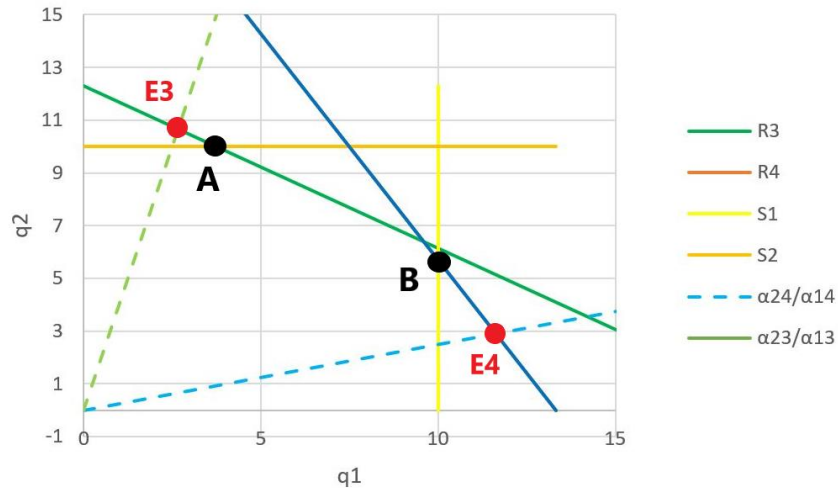


Figure 31. Stable solutions from node model with Equilibrium Theory

Both models have been computed in the intersection for a 30 minutes period with time intervals of 14.4 seconds. Regarding the continuous-time Markov chain, it has been assumed that flow ratios follow a normal distribution function with standard deviation  $\sigma = 3$ . Because of symmetry, results obtained in the horizontal corridor are very similar. For this reason, in this section only the origin-destination paths  $1 \rightarrow 3$  and  $2 \rightarrow 3$  will be compared for both models. Nevertheless, results for other origin-destinations are included in *Appendix D*.

Figure 32 and Figure 33 show density charts (number of vehicles per kilometer) for the traditional and the proposed model respectively. Traditional node model generates results almost identical for  $1 \rightarrow 3$  and  $2 \rightarrow 3$  paths. In Figure 32, the first 5km corresponds to the corridor 1 for the left figure and to the corridor 2 for the right one. The last 5km corresponds to the corridor 3. It can be observed that, while corridor 3 does not present congestion, corridors 1 and 2 start to present high densities since 0.1h. Specifically, this congestion starts in the intersection (which corresponds to 5km distance in the plot) and it propagates backwards the corridor.

Nevertheless, proposed model presents different densities for  $1 \rightarrow 3$  and  $2 \rightarrow 3$  paths. While corridor 1 reaches 200veh/km maximum density, corridor 2 has a small congestion around 50veh/km. This congestion starts around 0.1h for corridor 1 and around 0.15h for corridor 2, and it spills back through the links.

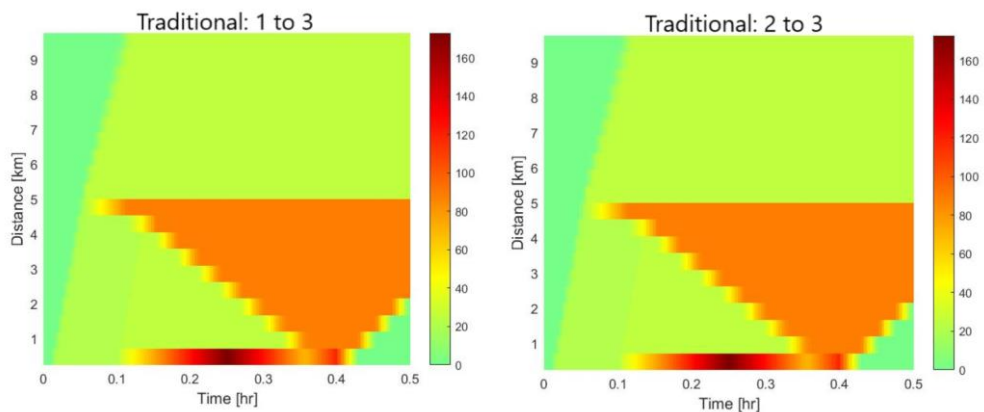


Figure 32. Density chart for the path 1 to 3 and 2 to 3 applying the traditional node model

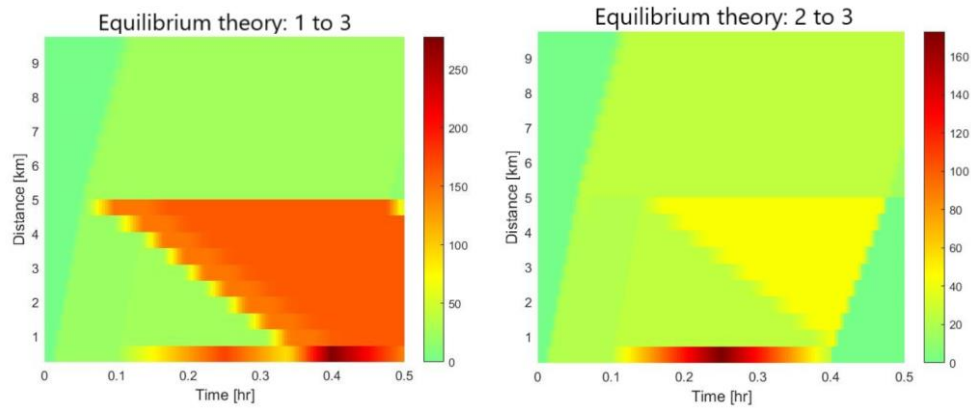


Figure 33. Density chart for the path 1 to 3 and 2 to 3 applying the proposed node model

The reason that the proposed model gives different densities for each path is because this model is able to consider all feasible solutions. The two stable solutions A ( $q_1 = 3.9$ ,  $q_2 = 10$ ) and B ( $q_1 = 10$ ,  $q_2 = 5.6$ ) identified by equilibrium theory are weighted by the Markov model to give a unique solution. Notice that B state is significantly closer to S than A state. This means that making a transition from B to A is significantly more probable than making a transition from A to B. Then, traffic flow will spend more time in A state than in B state. This reflection is directly translated to Figure 33: if A is the predominant solution, more flow will be sent from corridor 2 than from corridor 1 because  $q_{2_A} = 10 > q_{1_A} = 3.9$ .

Same reasoning can be done observing the flow charts (number of vehicles per hour) in Figure 34 and Figure 35. While traditional node model generates the same outputs for both  $1 \rightarrow 3$  and  $2 \rightarrow 3$  paths, equilibrium theory presents different behaviors. The area with yellow colour from left chart in Figure 35 represents congestion in corridor 1. On the contrary, right side chart from Figure 35 shows high flows from corridors 2 and 3 during all the computational time.

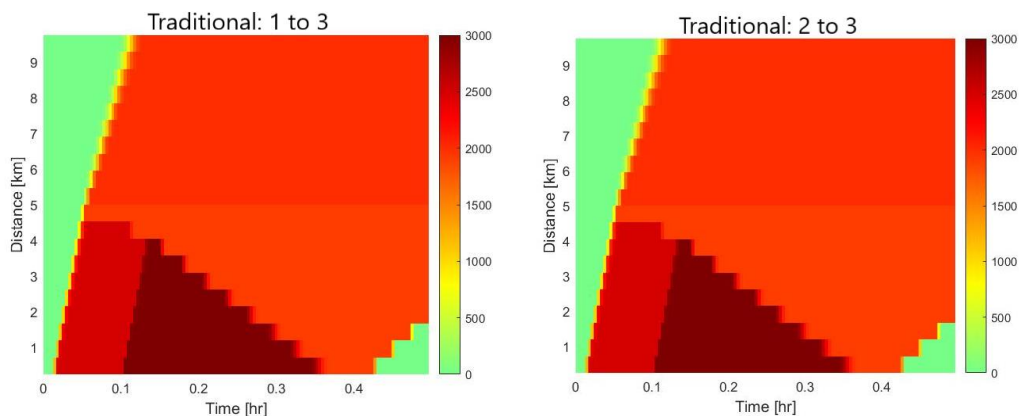


Figure 34. Flow chart for the path 1 to 3 and 2 to 3 applying the traditional node model

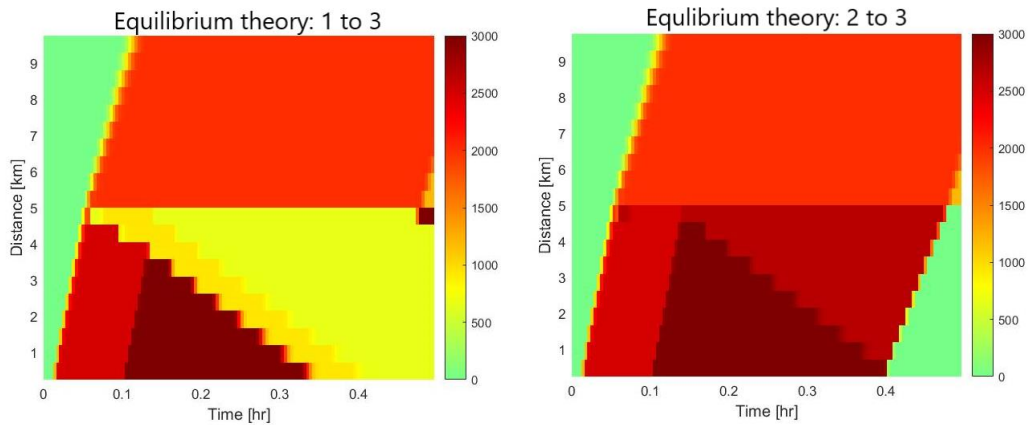


Figure 35. Flow chart for the path 1 to 3 and 2 to 3 applying the proposed node model

## 5 Concluding remarks

This thesis presents a model to deal with non-uniqueness issue in macroscopic first-order node models in the context of DNL. This model comprises two sections: an equilibrium theory which determines all the potential solutions, and a post-processing approach based on the continuous-time Markov chain model to find a realistic combination of possible solutions within an arbitrary time interval. DNL models do not consider stochasticity; thus, all the possible solutions should be combined to represent the expected flows at an intersection. To this end, the Markov model is implemented for finding the expected residual time in each possible situation. Then, expected flow at a node can be calculated.

The main contribution of this thesis is the Equilibrium Theory model: a completely new conceptual approach about how to determine all the non-unique solutions. It takes into account some crucial behavioral assumptions like the intersection between PRLs and constraints should not be considered as a possible solution, but more considerations are required. These considerations add more flexibility to the problem, allowing to reach uniqueness in some seemingly non-unique situations regarding traditional methods. The equilibrium theory algorithm has been developed for any 2-N dimension intersection (2 incoming links and N outgoing links/constraints). The extension of this approach to higher dimensions has been studied, but new obstacles could not be dealt with due to time scarcity.

Dealing with cases that include more than one potential solution regarding equilibrium theory has motivated the development of a new post-process approach based on the continuous Markov chain model. This post-process method follows similar behavioral assumptions applied in equilibrium theory. Flow ratios are not considered constant, but they follow a certain probability distribution which has been considered known through this thesis. Knowing the probability distribution of each solution, the Markov model generates a probability of residing in each. The model uses the residual time associated with each solution to perform a weighted average, resulting in calculating the final unique solution of the node model. This model has been computed for a 2-N case in which two feasible solutions exist after implementing the equilibrium theory. The extension to an M-N dimension case needs more considerations and effort which was not possible within the time scope of this thesis.

## 6 Future work

This thesis introduces some future works: calibrating the distribution functions already used in the presented model and extending the concept of equilibrium theory to M-N dimensions followed by the extension of the Markov model.

Empirical observations about non-uniqueness in complex intersections are an under-development field, and studies about how drivers behave in these situations is vital to tackle the problem realistically. Empirical studies in this field would provide rich insight for researchers in terms of estimating the probability distribution functions based on which the Markov model works.

On the other hand, generalization to M-N dimension is a relevant future work so the equilibrium theory and the Markov model can be implemented to solve any intersection with any arbitrary structure. For clarification of complexities associated with such a case, consider the intersection shown in 36 which follows the priority-to-the-right rule. This case generates non-uniqueness due to circular dependencies ( $P_{15} > P_{26} > P_{34} > P_{15}$ ) from all the movements. It actually represents a case in which one movement has priority in one of the conflicts in which it is involved and has to yield in the other.

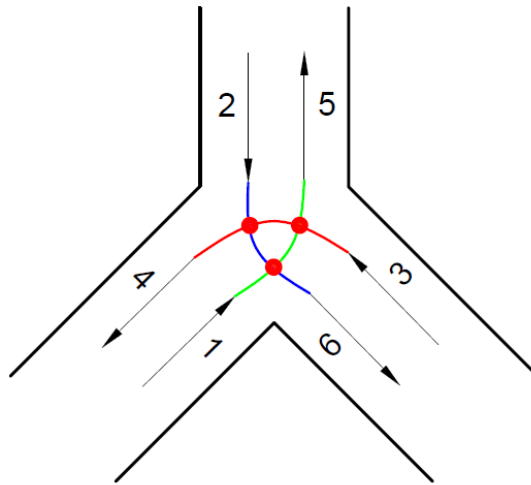


Figure 36. 3-3 dimensional intersection

The  $q$  plane of the considered example is a 3-dimensional space where each axis corresponds to the flow from an incoming link ( $q_1, q_2, q_3$ ). The intersect of PRL's with the corresponding constraint line is called  $E$  point ( $E_1, E_2$  and  $E_3$ ). For example,  $q_2$  yields to  $q_1$  with a certain ratio  $\frac{q_2}{q_1}$  because of priority-to-the-right rule resulting in  $E_1(a, b)$  point in the most upper left graph of Figure 37. Yet, there is the third dimension of  $q_3$  which needs to be included. Respecting the holding-free concept, the extension results in the point  $E_1(a, b, \infty)$ , shown in the most lower left of Figure 37. However, this point is not feasible and needs to be bounded by demand. The same reasoning holds for other attractors shown in Figure 37 ( $E_2$  and  $E_3$ ).

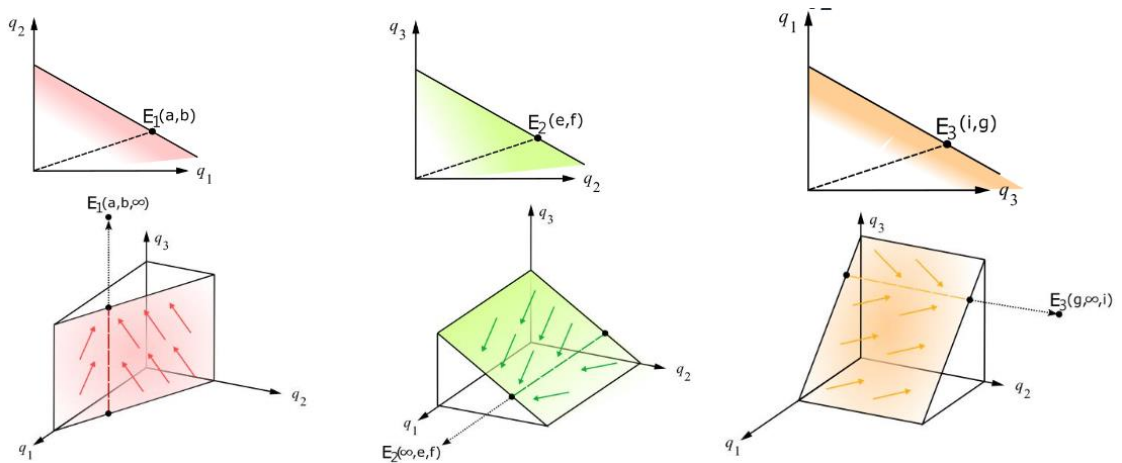


Figure 37. Attractor's representation in the 3 dimensional space (Tampère et al., 2018)

These constraints form a polyhedral with a certain shape, depending on the constraints and priority ratios. As in the 2-dimensional case, the 3-dimensional intersection can lead to uniqueness or non-uniqueness when applying Equilibrium Theory:

- Uniqueness: It occurs if all the attractors are located outside the feasible region. In 3D, attractors can be located in infinity if they do not intersect a supply constraint in this third dimension. Hence, if all attractors are located in infinity, chevrons in the feasible region will converge to a point  $S$  which can be determined with an adequate conventional node model (see left polyhedral from Figure 38).
- Non-uniqueness: It occurs if at least one attractor is located inside the feasible region. If an attractor intersects a supply constraint in the third dimension, this attractor will be located inside the feasible area. This means that chevrons from this plane will point to the attractor instead of the convergence point  $S$ . In the right polyhedral from Figure 38, all three attractors are located inside the feasible region. Thus, equilibrium theory suggests non-uniqueness with three possible candidates.

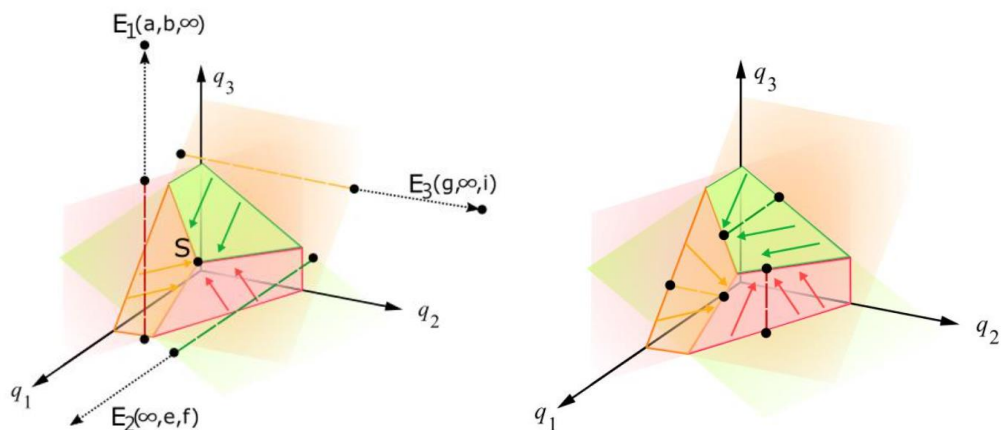


Figure 38. (a) Equilibrium Theory converges in a unique point  $S$ ; (b) Equilibrium Theory presents non-uniqueness with three candidates (Tampère et al., 2018)

Furthermore, equilibrium theory in a 3-M case can be tricky. Suppose that after applying equilibrium theory, chevrons determine two possible candidates: a convergence point  $S$  and an attractor  $E_1$ , both located in the same edge of the polyhedral. Following the equilibrium theory mechanisms, the section between  $S$  and  $E_1$  would present chevrons with opposite directions. This is because the edge is originated from the intersection of two constraint planes, thus, chevrons from one plane will point to  $S$  while chevrons from the other plane will point to  $E_1$ . Zones with opposite chevrons' directions are not considered by equilibrium theory, for this reason this is a field that calls for further developments.

## 7 Appendix

### 7.1 Appendix A

This appendix shows the pseudo-code for the application of the Equilibrium Theory.

```

If nbOutgoingLinks > 1
· If any(sendingFlowi > receivingFlowj) && any(sendingFlowi' >
receivingFlowj)  $\forall i \neq i'$ 
· · function(Feasible set)
· · p = 0
· · for i = 1:length(Intersections(:,1))
· · · q1 = Intersections(i,1)
· · · q2 = Intersections(i,2)
· · · if q1 ≤ sendingFlow(1)
· · · · if q2 ≤ sendingFlow(2)
· · · · · if q1 ≥ 0
· · · · · if q2 ≥ 0
· · · · · · r = 0
· · · · · · for j = 1:nbOutgoingLinks
· · · · · · · if q2 ≤ (receivingFlow(j) - turningFractions(1,j)
· · · · · · · · q1)/turningFractions(2,j)
· · · · · · · · r = r + 1
· · · · · · · if r == nbOutgoingLinks
· · · · · · · · p = p + 1
· · · · · · · · envelope(p,1) = Intersections(i,1)
· · · · · · · · envelope(p,2) = Intersections(i,2)
· · · · · · · end
· · · · · · end
· · · · · end
· · · · end
· · · end
· · end
· · p = 0
· · for i = 1:length(envelope(:,1))
· · · if envelope(i,:) == any(attractor)
· · · · solution(p,:) = envelope(i,:)
· · · end
· · end
· · for i = 1

```

Check sufficient non-uniqueness conditions

Compute intersection points

For each intersection point

Check S1 constraint  
Check S2 constraint  
Check positive y axis  
Check positive x axis

Check all supply constraints

If all constraints are fulfilled, the point belongs to the envelope

For each envelope point  
If any envelope point is an attractor  
This point is a stable solution

For the first demand constraint

```

... for j = nbOutgoingLinks
... if q2 == (receivingFlow(j) - turningFractions(1,j)
             * q1)/turningFractions(2,j)
... if any(envelope) == (i,j)
... if i < Attractor(j,1)
... p = p + 1
... solution(p,:) = [i,j]
... end
... end
... end
... end
.. for i = 2
... for j = nbOutgoingLinks
... if q2 == (receivingFlow(j) - turningFractions(1,j)
             * q1)/turningFractions(2,j)
... if any(envelope) == (i,j)
... if j < Attractor(j,2)
... p = p + 1
... solution(p,:) = [i,j]
... end
... end
... end
... end
.. for k = 1:length(envelope(:,1))
.. for i = 1:nbOutgoingLinks
.. for j = 1:nbOutgoingLinks
... if i ≠ j
... Sx = (receivingFlow(i) * turningFractions(2,j)
          - receivingFlow(j)
          * turningFractions(2,i))/(turningFractions(1,i)
          * turningFractions(2,j) - turningFractions(1,j)
          * turningFractions(2,i));
... Sy = (receivingFlow(i) - Sx
          * turningFractions(1,i))/turningFractions(2,i);
... if Sx = envelope(k,1) && Sy = envelope(k,2)
... if Sx < Attractor(i,1)
... if Sx > Attractor(j,1)
... p = p + 1
... solution(p,:) = envelope(k,:)
... end
... end
... end
... end
... end
.. if length(solution(:,1)) == 1
.. TurnFlows = turningFractions.* solution'
.. elseif length(solution(:,1)) > 1

... function(Markov Chain)
.. end
.. end
end

```

For each supply constraint  
If it exists an intersection point  
between both constraints  
If it belongs to the feasible envelope  
If attractor is outside feasible region

This point is a stable solution

For the second demand constraint  
For each supply constraint  
If it exists an intersection point  
between both constraints  
If it belongs to the feasible envelope  
If attractor is outside feasible region

This point is a stable solution

For each envelope point  
For each supply constraint i  
For each supply constraint j  
If these constraints are not the same  
Horizontal coordinate of the  
intersection point between supply  
constraints

Vertical coordinate

To know which supply constraints act  
If first chevrons point to intersection  
Analyse second chevrons

This point is a stable solution

If there is one stable solution

If there are more than one stable  
solution  
Apply post-processing method

Pseudo-code for computing feasible set:

<pre> function(Feasible set) · p = 0 · for i = 1:nbOutgoingLinks · · Intersections(p,1)           = receivingFlow(i)             * priorities(1,i)/(turningFractions(1,i) * priorities(1,i)             + turningFractions(2,i) * priorities(2,i)) · · Intersections(p,2) = Intersections(p,1) * priorities(2,i)/priorities(1,i) · end · for i = 1:nbOutgoingLinks · · for j = 1:nbOutgoingLinks · · · if i ≠ j · · · · p = p + 1 · · · · Intersections(p,1)           = (receivingFlow(i) * turningFractions(2,j)             - receivingFlow(j)             * turningFractions(2,i))/(turningFractions(1,i)             * turningFractions(2,j) - turningFractions(1,j)             * turningFractions(2,i)) · · · · Intersections(p,2)           = (receivingFlow(i) - Intersections(p,1)             * turningFractions(1,i))/turningFractions(2,i) · · · end · · end · end · for i = 1:nbOutgoingLinks · · p = p + 1 · · Intersections(p,1) = sendingFlow(1) · · Intersections(p,2)           = (receivingFlow(i) - sendingFlow(1)             * turningFractions(1,i))/turningFractions(2,i) · end · for i = 1:nbOutgoingLinks · · p = p + 1 · · Intersections(p,1)           = (receivingFlow(i) - sendingFlow(2)             * turningFractions(2,i))/turningFractions(1,i) · · Intersections(p,2) = sendingFlow(2) · end end </pre>	<p style="text-align: right;">Start function</p> <p>For each supply constraint, calculate intersection point with each PRL</p> <p>For each supply constraint i For each supply constraint j Being different constraints</p> <p>Calculate intersection point between supply constraints</p> <p>For each supply constraint</p> <p>Calculate intersections between supply constraint and demand constraint S1</p> <p>For each supply constraint</p> <p>Calculate intersections between supply constraint and demand constraint S2</p>
--	--

## 7.2 Appendix B

Continuous-time Markov chain pseudo-code:

<pre> function(Markov Chain) · if length(solution(:,1)) &gt; 1 · · for i = 1:length(solution(:,1)) · · · slope = solution(i,2)/solution(i,1) · · · xslope(i,:) = slope - 10:0.1:slope + 10 </pre>	<p style="text-align: right;">Start function</p> <p>If there is non-uniqueness For each stable solution Calculate slope Determine function range, e.g. [mean-10, mean+10]</p>
---	---

```

... yslope(i,:) = normpdf(xslope(i,:),slope,3)
... interalpha = min(abs(xslope(i,:) - (Sy/Sx)))
... alpha(i) = sum(yslope(i,interalpha:end))
.. end
.. a = alpha(1)/(alpha(1) + alpha(2))
.. b = alpha(2)/(alpha(1) + alpha(2))
.. t = dt * 3600
.. TransMatrix(1,1) = b + a * exp(-(alpha(1) + alpha(2)) * t)
.. TransMatrix(1,2) = a - a * exp(-(alpha(1) + alpha(2)) * t)
.. TransMatrix(2,1) = b - b * exp(-(alpha(1) + alpha(2)) * t)
.. TransMatrix(2,2) = a + b * exp(-(alpha(1) + alpha(2)) * t)
.. K(1,1) = solution(i,1) * (1 + TransMatrix(i,1))
.. K(1,2) = solution(i,2) * (1 + TransMatrix(i,2))
.. end
.. TurnFlows = turningFractions.*K'
end

```

Perform probability function, e.g. normal distribution with standard deviation 3  
Find intersection with S  
Obtain area alpha/beta

Calculate probability transition matrix

Calculate weighted flow average K

Obtain final flow distribution

### 7.3 Appendix C

Appendix B shows the results from the transition probability matrix  $P(t)$  for different time periods. The time period analysed is  $t \in [0,10]$ . The results are shown below:

Table 3. Transition probability matrix results from example 1

t	P(1,1)	P(1,2)	P(2,1)	P(2,2)
0	1	0	0	1
0.5	0.8523395	0.1476605	0.06707063	0.93292937
1	0.7363863	0.2636137	0.1197391	0.8802609
1.5	0.64533187	0.35466813	0.16109802	0.83890198
2	0.57382965	0.42617035	0.19357588	0.80642412
2.5	0.51768119	0.48231881	0.21907974	0.78092026
3	0.47358955	0.52641045	0.23910713	0.76089287
3.5	0.43896576	0.56103424	0.25483401	0.74516599
4	0.41177677	0.58822323	0.26718384	0.73281616
4.5	0.39042611	0.60957389	0.27688178	0.72311822
5	0.3736601	0.6263399	0.28449727	0.71550273
5.5	0.36049427	0.63950573	0.29047748	0.70952252
6	0.35015556	0.64984444	0.29517355	0.70482645
6.5	0.34203689	0.65796311	0.29886123	0.70113877
7	0.33566155	0.66433845	0.30175705	0.69824295
7.5	0.33065519	0.66934481	0.30403104	0.69596896
8	0.32672385	0.67327615	0.30581674	0.69418326
8.5	0.3236367	0.6763633	0.30721899	0.69278101
9	0.32121245	0.67878755	0.30832014	0.69167986
9.5	0.31930877	0.68069123	0.30918483	0.69081517
10	0.31781386	0.68218614	0.30986385	0.69013615

Table 4. Transition probability matrix results from example 2

t	P(1,1)	P(1,2)	P(2,1)	P(2,2)
0	1	0	0	1
0.5	0.89579935	0.10420065	0.10420065	0.89579935
1	0.81331426	0.18668574	0.18668574	0.81331426
1.5	0.74801916	0.25198084	0.25198084	0.74801916
2	0.69633165	0.30366835	0.30366835	0.69633165
2.5	0.65541588	0.34458412	0.34458412	0.65541588
3	0.62302701	0.37697299	0.37697299	0.62302701
3.5	0.59738802	0.40261198	0.40261198	0.59738802
4	0.57709223	0.42290777	0.42290777	0.57709223
4.5	0.56102611	0.43897389	0.43897389	0.56102611
5	0.54830819	0.45169181	0.45169181	0.54830819
5.5	0.5382407	0.4617593	0.4617593	0.5382407
6	0.53027129	0.46972871	0.46972871	0.53027129
6.5	0.52396271	0.47603729	0.47603729	0.52396271
7	0.51896885	0.48103115	0.48103115	0.51896885
7.5	0.51501572	0.48498428	0.48498428	0.51501572
8	0.51188642	0.48811358	0.48811358	0.51188642
8.5	0.50940928	0.49059072	0.49059072	0.50940928
9	0.50744837	0.49255163	0.49255163	0.50744837
9.5	0.50589612	0.49410388	0.49410388	0.50589612
10	0.50466736	0.49533264	0.49533264	0.50466736

## 7.4 Appendix D

This appendix presents some extra information from the modelled example in *Solution with proposed node model* section. The incoming flow in function of time for each origin-destination is presented in Figure 39 and Figure 40 .

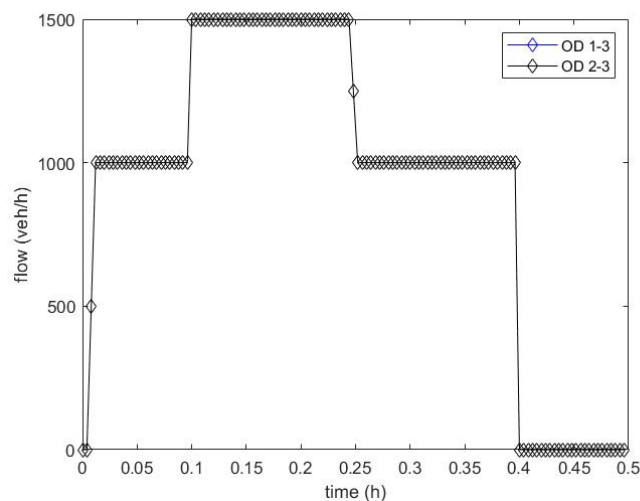


Figure 39. Incoming flow in function of time with destination 3

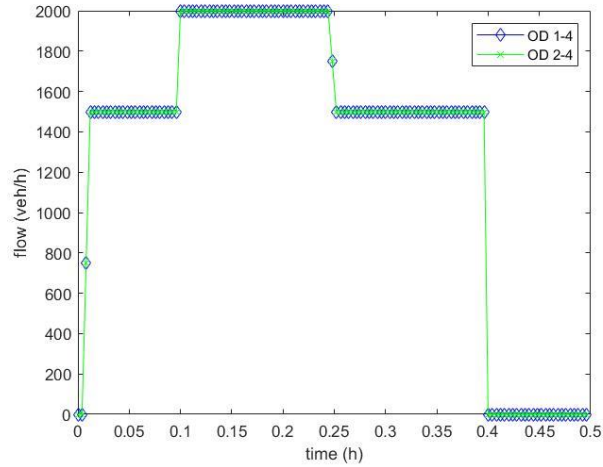


Figure 40. Incoming flow in function of time with destination 4

Density charts for the rest of origin-destinations are showed in Figure 41 and Figure 42. Finally, flow charts for the rest of origin-destinations are showed in Figure 41 and Figure 42.

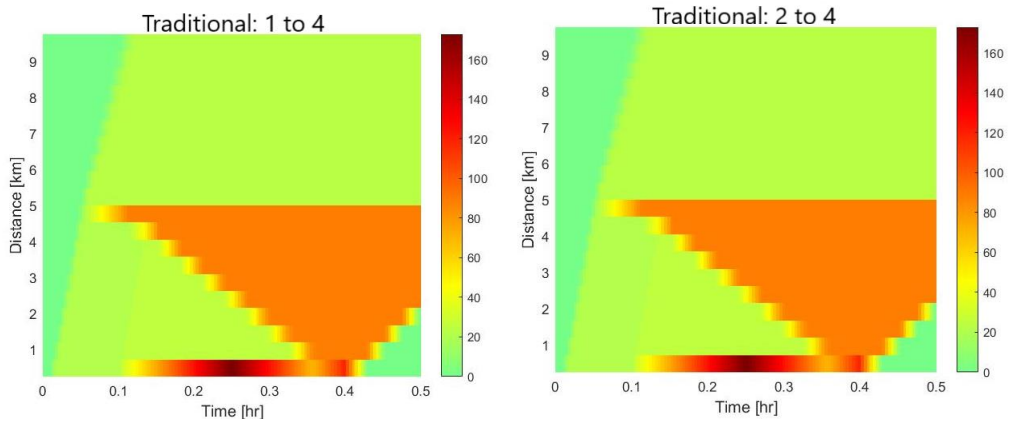


Figure 41. Density chart for the path 1 to 4 and 2 to 4 applying the traditional node model

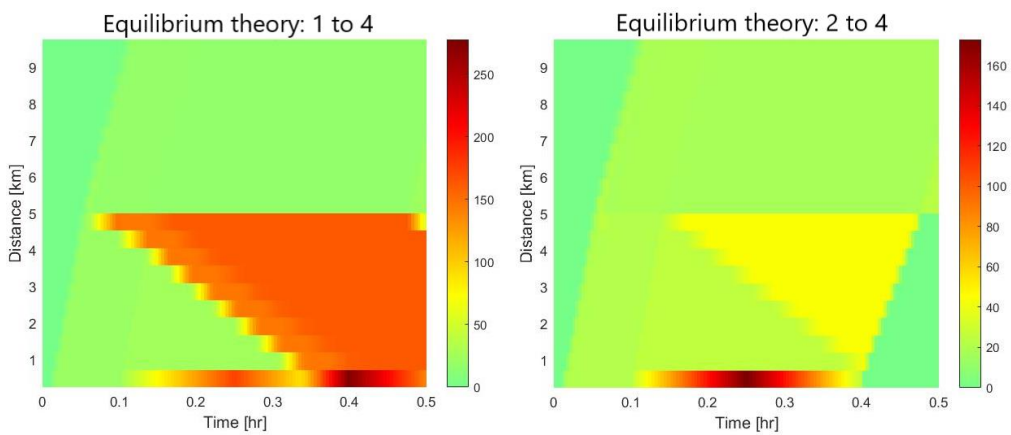


Figure 42. Density chart for the path 1 to 4 and 2 to 4 applying equilibrium theory

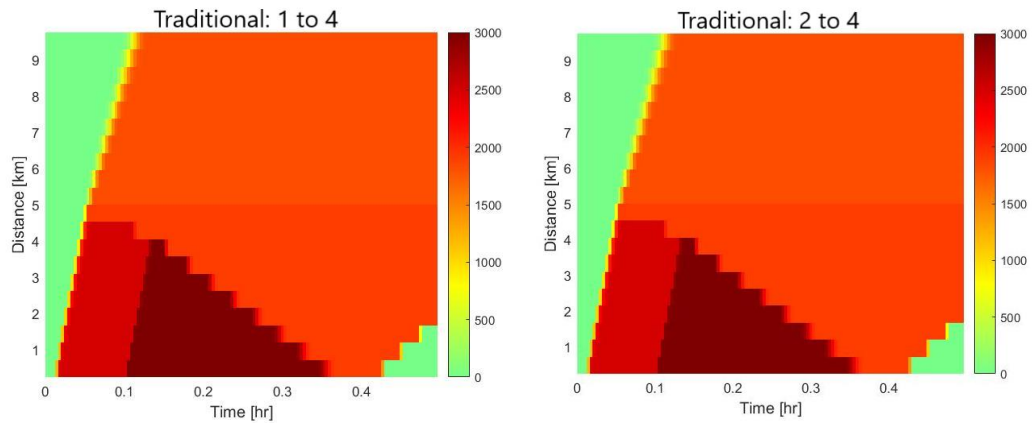


Figure 43. Flow chart for the path 1 to 4 and 2 to 4 applying the traditional node model

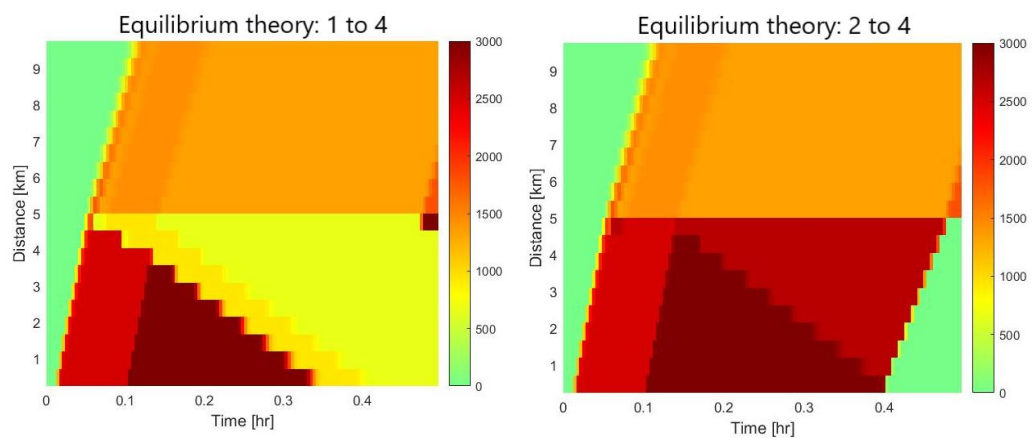


Figure 44. Flow chart for the path 1 to 4 and 2 to 4 applying equilibrium theory

## 8 References

- Bar-Gera, H., & Ahn, S., 2010. Empirical macroscopic evaluation of freeway merge-ratios. *Transportation Research Part C: Emerging Technologies*, 18(4), 457-470.
- Corthout, R., Flötteröd, G., Viti, F., Tampère, C.M., 2012. Non-unique flows in macroscopic first-order intersection models. *Transportation Research Part B: Methodological* 46 (3), 343–359.
- Daganzo, C.F., 1995. The cell transmission model part II: network traffic. *Transportation Research Part B* 29 (2), 79-93.
- Flötteröd, G., Rohde, J., 2011. Operational macroscopic modeling of complex urban road intersections. *Transportation Research Part B* 45, 903-922.
- Gentile, G., Meschini, L., & Papola, N., 2007. Spillback congestion in dynamic traffic assignment: a macroscopic flow model with time-varying bottlenecks. *Transportation Research Part B: Methodological*, 41(10), 1114-1138.
- Gibb, J., 2011. Model of traffic flow capacity constraint through nodes for dynamic network loading with queue spillback. *Transportation Research Record: Journal of the Transportation Research Board* 2263 (-1), 113–122.
- Jabari, S.E., 2016. Node modeling for congested urban road networks. *Transportation Research Part B* 91, 229–249.
- Jin, W. L., and Zhang, H. M., 2003. On the distribution schemes for determining flows through a merge. *Transportation Research Part B: Methodological*, 37(6), 521-540.
- Kalai, E., and Samet D., 1985. Unanimity games and Pareto optimality. *International Journal of Game Theory* 14, 41-50.

- Lebacque, J., Khoshyaran, M., 2005. First order macroscopic traffic flow models: intersections modeling, network modeling. In: Proceedings of the 16th ISTTT.
- Leclercq, L., Laval, J. A., & Chiabaut, N. (2011). Capacity drops at merges: An endogenous model. *Transportation Research Part B: Methodological*, 45, 1302-1313.
- Ni, D., and Leonard, J. D., 2005. A simplified kinematic wave model at a merge bottleneck. *Applied Mathematical Modelling*, 29(11), 1054-1072.
- Smits, E.S., Bliemer, M. C.J, Pel, A. J., van Arem, B., 2015. A family of macroscopic node models. *Transportation Research Part B: Methodological* 74(1) 20–39.
- Tampère, C.M.J., Corthout, R., Cattrysse, D., Immers, L.H., 2011. A generic class of first order node models for dynamic macroscopic simulation of traffic flows. *Transportation Research Part B* 45 (1), 289-309.
- Tampère, C.M.J., Himpe, W., Yahyamoazarani, R., 2018. Non-unique flows in macroscopic first-order intersection models – An equilibrium theory.
- TanChen, Y. H., 2017. Some Notes on Geometric Interpretation of Holding-Free Solution for Urban Intersection Model, Manuscript (arXiv:1702.00593).